REPORT DOCUMENTATION PAGE	AFRL-SR-BL-TR-02-0113

1. AGENCY USE ONLY (*Leave Blank*)	2. REPORT DATE 15 July 2000	3. REPORT TYPE AND DATES COVERED Interim Quarterly Report

TITLE AND SUBTITLE
Forecasting Heliospheric Structure Using the Solar Mass Ejection Imager (SMEI)

5. FUNDING NUMBERS
PR AF49620-98-1-0062

6. AUTHORS
Bernard V. Jackson, Andrew Buffington, P. Paul Hick and David F. Webb

7. PERFORMING ORGANIZATION NAME(S) AND ADDRESS(ES)
The Regents of the University of California
University of California, San Diego

8. PERFORMING ORGANIZATION REPORT NUMBER
Final

9. SPONSORING / MONITORING AGENCY NAME(S) AND ADDRESS(ES)
Dr. Paul Bellaire
Program Manager, Space & Upper Atmospheric Sciences
Air Force Office of Scientific Research
801 N. Randolph Street, Rm 732
Arlington VA 22203-1977

10. SPONSORING / MONITORING AGENCY REPORT NUMBER

11. SUPPLEMENTARY NOTES

12a. DISTRIBUTION / AVAILABILITY STATEMENT
UNLIMITED

13. ABSTRACT *(Maximum 200 words)*
Solar disturbances produce major effects in the corona, its extension into the interplanetary medium, and ultimately, the Earth's environment. The ability to forecast the arrival at Earth of these disturbances and to determine their effects on the geospace environment is of primary interest to the Air Force, which communicates through and maintains satellites within this environment. We have developed imaging and other techniques for use in mapping these disturbances (mainly coronal mass ejections or CMEs) as they move away from the Sun. This capability has begun to revolutionize the study of large-scale heliospheric space plasma interactions. The Solar Mass Ejection Imager (SMEI), now being developed and constructed, will have an angular and temporal resolution far better than the data sets (interplanetary scintillation and Thomson scattering observations from the HELIOS photometers) for which our imaging techniques were originally developed. SMEI will produce a thousand times as much data as previously available, exceeding our current data analysis capabilities. The development of adequate analysis and modeling techniques for SMEI data is a serious challenge, which must be addressed in order to maximize the scientific return from the SMEI mission, in particular with respect to our ability to accurately forecast the arrival of heliospheric disturbances at Earth.

14. SUBJECT TERMS			15. NUMBER OF PAGES 37
			16. PRICE CODE
17. SECURITY CLASSIFICATION OF REPORT UNCLASSIFIED	18. SECURITY CLASSIFICATION OF THIS PAGE UNCLASSIFIED	19. SECURITY CLASSIFICATION OF ABSTRACT UNCLASSIFIED	20. LIMITATION OF ABSTRACT UL

NSN 7540-01-280-5500

Standard Form 298 (Rev. 2-89)
Prescribed by ANSI Std. Z39-1

Forecasting Heliospheric Structure Using the Solar Mass Ejection Imager (SMEI)

I. Introduction

The outermost parts of the solar atmosphere - the corona and solar wind - experience dramatic perturbations related to flares and mass-ejection transients. These disturbances extend to the Earth's magnetosphere and to Earth itself. In the past, observations of the origins of these disturbances in the lower corona have been restricted to coronal emission-line observations and the meter-wave radio band, but since the 1970's we have seen the addition of powerful new observing tools for observation: sensitive coronagraphs, both in space and at terrestrial observatories; X-ray imaging telescopes; low-frequency radio telescopes; space-borne kilometric wave radio receivers; and interplanetary scintillation data.

The primary object of earlier research has been to understand the physics and spatial extents of heliospheric structures such as coronal mass ejections and streamers. In comparison with spacecraft *in situ* and ground-based data, this leads to a better determination of the total mass and energy of these structures. In addition, we have addressed the question of how easy these features are to observe and how we can forecast their effects at Earth. This study has resulted primarily from analyzing the data from the zodiacal light photometers on board the HELIOS spacecraft.

We describe our recent results on HELIOS photometer observations of mass ejections, corotating density enhancements and other heliospheric features partially supported by previous AF grants titled 'Remote Sensing of Inner Heliospheric Plasmas', and 'The Physics of Remotely-Sensed Heliospheric Plasmas' in Section II of this report. The new research section (Section III) emphasizes the studies we have begun under the current contract 'Forecasting Heliospheric Structure Using the Solar Mass Ejection Imager (SMEI)' and concludes with a list of papers as well as a list of the personnel that have been supported by *this* contract. Section IV states the future goals of the project. Conclusions and an executive summary of the analysis to be performed in the next year are presented in Section V.

II. Scientific Background and Recent Results

The Sun emits clouds of ionized gas and entrained magnetic fields ("coronal mass ejections or CMEs") and hydrodynamic disturbances ("shock waves") which are responsible for most sudden commencements and magnetic storms occurring at the Earth. CMEs are the most dramatic disturbances of the heliosphere and the ones first detected in the HELIOS photometer data (Richter *et al.*, 1982). As shown by Webb *et al.* (1980), the mass ejecta at the time of a solar flare may be more important energetically than its other manifestations in the lower solar atmosphere. Thus, it is imperative to study the masses and 3-dimensional structures of the mass ejections in order to understand the flare process. This provides an additional incentive for the study of mass ejection phenomena, over and above our interest in the physical mechanisms involved in the acceleration of mass and particles associated with the mass motions themselves.

In the lower corona the major mass ejections observed in Hα are termed "eruptive prominences," and are typically associated with a particular kind of flare characterized by two

expanding bright ribbons in the chromosphere and a growing system of hot coronal loops rooted in these ribbons (*e.g.*, Švestka, 1986). The X-ray loops appear to move gradually upward in a steady sequence of diminishing temperature and velocity, and their emission decays with time scales of hours (*e.g.*, Švestka, 1981). These long-duration X-ray events (Kahler, 1977; Sheeley *et al.*, 1983) are well-associated with the ejection of mass into the corona (CMEs), the acceleration of interplanetary protons (Kahler *et al.*, 1978), and meter-wave radio phenomena (Webb and Kundu, 1978).

The quantitative study of mass ejections essentially began with the Skylab coronagraph (*e.g.*, Rust and Hildner *et al.*, 1980), and has been greatly enhanced by the advent of new coronal instruments. There are data available from the P78-1 and SMM spacecraft, and from mountaintop observatories such as Sacramento Peak and Mauna Loa. Coronagraph observations of CMEs are most sensitive to those events which move outward above the limb of the Sun. Occasionally, some CMEs can be observed to partially surround the Sun (like a 'halo') (Jackson, 1985a), and are interpreted as either moving towards (or away from) the Earth. Recently, *e.g.*, on January 6 and February 7, 1997, two such CMEs were observed by the LASCO coronagraph instruments on the SOHO spacecraft and were forecast to arrive at Earth (Webb, 1997a, b) where they were associated with magnetic clouds and geomagnetic storms.

The Thomson-scattering CME observations from the HELIOS spacecraft photometers (Leinert *et al.*, 1981) provide a link between coronal observations and those obtained *in situ* in the heliosphere. These observations have been used to map CMEs to elongations (angular distances from the Sun) which extend from 15° to as great as 165°. Such global observations over a large range of elongations can unambiguously determine whether or not CMEs are heading towards the Earth and provide accurate determinations of their arrival times.

CMEs originate in the lower corona in closed magnetic field configurations (beneath streamers, *e.g.*, Jackson, 1981). It is generally assumed (and confirmed by coronagraph observations for the rise of the CME over the first few solar radii) that the closed topology is maintained as the CME moves outward into the heliosphere. Magnetic field lines (generally described as magnetic 'bottles', loops or flux ropes) expand outward, but remain rooted with both footpoints in the Sun. In some cases reconnection may lead to the formation of a magnetic structure completely detached from the Sun and convecting outward embedded in the solar wind (a 'plasmoid').

The most energetic CME events, with propagation velocities significantly higher than the ambient solar wind, drive shock waves ahead of them. Most results on interplanetary signatures of CMEs are derived from the search for 'unusual' (as compared to the undisturbed solar wind) particle, plasma and/or magnetic properties of the solar wind plasma behind these interplanetary shocks. Several unusual signatures have been identified for these shock-associated events (see *e.g.*, Schwenn, 1986; Gosling, 1990), such as high magnetic field strength, low temperature, gradual rotation (over many hours) of the magnetic field vector over large angles, low magnetic field variance, low plasma beta and high He abundance. It seems reasonable to expect that some of these signatures will continue to be present when less-energetic CMEs, moving too slowly to cause the formation of a shock, move past a spacecraft in the inner heliosphere. Probably the best indication of the passage of a CME is the passage of a magnetic cloud structure showing the first three signatures (high field strength, low temperature, large coherent rotation; Burlaga, 1991). However, magnetic clouds are probably only a subset of the much broader class of all CME events (*e.g.*, see Jackson, 1997).

An additional source of information about heliospheric disturbances is interplanetary scintillation (IPS) observation from meter-wave intensity variations of point radio sources. These data have long been used to measure small-scale (~200 km) heliospheric density variations along the line of sight to the source (Hewish *et al.*, 1964, Ananthakrishnan *et al.*, 1980). These observations are also global and can be used to unambiguously map heliospheric disturbances headed towards the Earth, generally with a daily temporal cadence.

IPS observations can highlight heliospheric disturbances of large scale that change from one day to the next and are often associated with geomagnetic storms on Earth, such as CMEs (Gapper *et al.*, 1982). IPS observations from the Cambridge, England, array (Houminer, 1971) show a predominance of disturbances that appear to corotate with the Sun as inferred from the list of events and their associations (Hewish and Bravo, 1986). On each day it is possible to determine an approximate size and shape of the structures that move past Earth beyond ~50° (≥0.75 AU). These features, presumably modified significantly by their passage through the interplanetary medium on the way to 1 AU, can be classified as structures that are either corotating or detached from the Sun (*e.g.*, Behannon *et al.*, 1991).

These analyses are of interest to the Air Force for several reasons:

- The Air Force Research Laboratory, in conjunction with UCSD, Boston College and the University of Birmingham, England, is planning to place an Earth orbiting Solar Mass Ejection Imager (SMEI) in space as a proof-of-principle experiment to forecast the arrival at Earth of CMEs, heliospheric shocks and corotating dense regions. This instrument has been built and delivered in preparation for a 2002 launch. We are developing a data analysis system that can effectively deal with the large amounts of imaging data that will be returned from this instrument.

- The data from the HELIOS spacecraft photometers, which are most like the data that will be obtained from the Earth-orbiting SMEI imager, provide a valuable test-bed for data analysis procedures and imaging techniques to be used in the processing of SMEI observations. To demonstrate these techniques, we have also utilized existing IPS observations available from Nagoya, Japan and scintillation-level measurements from other IPS stations. These ground-based data are important in helping understand SMEI observations. Through our analyses of the IPS data we will maintain our collaborative effort with the groups providing these data and share their forecasting expertise.

The ability to observe the outward propagation of structures from the Sun allows researchers to understand how to forecast their arrival at Earth. This in turn leads to both a better understanding of how these features interact with the Earth's environment and how to forecast their effects on military and civilian space and communication systems. The understanding of these processes in the heliosphere and the near-Earth environment are particularly important to the Air Force which maintains many space assets including astronauts on the Space Shuttle and at the ISS.

II.A. The Solar Mass Ejection Imager (SMEI)

UCSD, Boston College and the University of Birmingham, England, in conjunction with the Air Force Research Laboratory have constructed and delivered the Solar Mass Ejection Imager (SMEI). This instrument (Jackson *et al.*, 1989; 1991; 1995; 1997b; Keil *et al.*, 1996) was originally designed

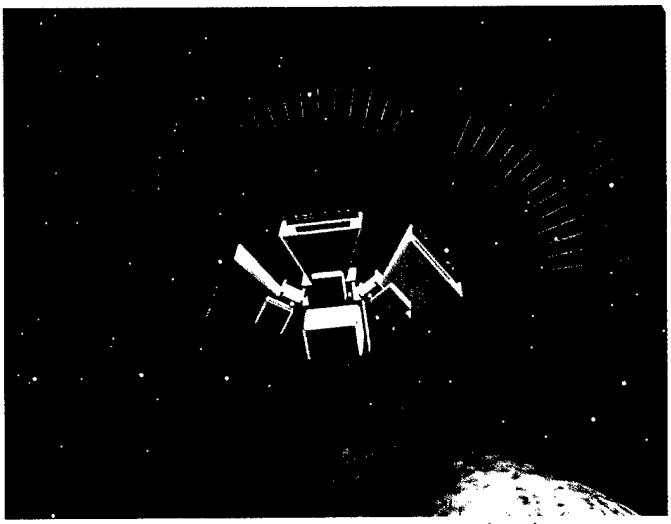

Fig. 1. Depiction of the Solar Mass Ejection Imager in polar orbit.

to operate in a mode similar to that of the HELIOS spacecraft photometers. Data from HELIOS was used to measure CMEs at solar distances of nearly 1 AU, proving that SMEI in Earth orbit will be able to detect and measure such structures. The instrument currently being constructed is to be placed in an Earth-terminator, Sun-synchronous orbit at ~850 km during the later half of 2002. Figure 1 is a schematic depiction of SMEI in polar orbit. The overall configuration of SMEI has progressed over a period of more than a decade. UCSD has been responsible for the overall preliminary design of the instrument, early baffle design and baffle prototype development and CCD testing, and more recently CCD selection, optics construction and instrument performance following integration onto the Coriolis spacecraft bus designed by Spectrum Astro, Inc.

At present we have no effective capability to track interplanetary disturbances within the gap between coronagraph observations within 30 Rs above the Sun until they impinge on the Earth's environment at 1 AU. SMEI will provide this capability and allow us to detect and track CMEs and other transient heliospheric structures as they move outward from the Sun with a time resolution of the spacecraft orbit, ~100 min. SMEI will also allow us to determine important physical parameters of CMEs and other heliospheric structures such as mass, density, speed, and location in space. These parameters can then be used to determine the extent to which these structures will affect the magnetosphere of Earth.

The SMEI CCD analysis and optics development currently underway at UCSD make it imperative that we develop the algorithms necessary to provide SMEI data to the rest of the community. The problems inherent in the SMEI design require that we analyze each section of sky to high photometric accuracy. The SMEI design stipulates that the SMEI photometric specification be no worse than 0.1% for any one square degree of sky on each orbit. This accuracy is dictated by the signal strength of CMEs and other heliospheric features, which average about 1 S10 unit (the intensity of one solar-type star with a magnitude of 10 per square degree of sky) at 90° elongation, but are several hundred times fainter than the zodiacal cloud and stars.

The first requirement for the SMEI instrument is that the signal to noise be sufficiently high as to measure the heliospheric plasma brightness relative to the other much brighter signals present in the images. The brightness distribution of the zodiacal cloud is nearly structureless and unchanging and, thus, we expect to remove its contribution by simple modeling and averaging techniques using a Sun-based ecliptic coordinate reference system. At times comets, and their dust or dust bands at the location of comet orbits, will be present in the data at different locations. However, since these spatially large and variable dust brightness signals did not significantly effect the HELIOS photometer data, we do not expect that they will hamper SMEI observations.

Stellar signals are another matter. Each square degree of sky has on average brightness from stars of over 100 S10 units. As bright points, stars must be located in each image and their effects subtracted on an image by image basis using a sidereal coordinate reference system. While stellar

positions to 14th magnitude (sufficient for removal from SMEI data) are now known, the brightnesses of stars, bright galaxies and nebulae as measured by the SMEI CCD systems, are not. To remove these stellar-like objects, we intend to register each location in the sky and to map this in intrinsic brightness. We have determined that it will be sufficient to register each four-second SMEI image within 0.001 degrees in order to remove the effects of point-like objects. We have also determined that each SMEI 3° by 60° field of view will have enough bright stars to permit this registration. We plan to provide the initial point-source map calibrated to the SMEI CCD response using an initial ground-based catalog over a large extent of the sky. We have developed a CCD flat field from each flight camera unit to about 1%, a factor of ten greater than the ultimate goal of 0.1%. We now know how much this map will be affected by the shapes of stellar images that change as they traverse the SMEI field of view. We have also devised a technique by which we can update this map iteratively to provide an accurate on-orbit catalog as well as a flat field from each flight unit to the required 0.1% accuracy.

Also required for SMEI image reduction will be analysis routines to remove the effects of cosmic rays and other rapidly time-varying signals from the data. There is no plan for a cosmic ray removal capability to be present on board the spacecraft. Thus, we have devised a cosmic ray removal algorithm that can prepare SMEI data for heliospheric analysis once the data are available on the ground.

II.B. HELIOS Photometer Data

As noted, the Thomson-scattering data from the HELIOS spacecraft are the most similar to those expected from SMEI. The HELIOS spacecraft, the first launched into heliocentric orbit in 1974, contained sensitive zodiacal-light photometers (Leinert *et al.*, 1981). Each of the two HELIOS spacecraft contained three photometers for the study of the zodiacal-light distribution. These photometers, at 16°, 31°, and 90° ecliptic latitude, swept the celestial sphere to obtain data fixed with respect to the solar direction, with a sample interval of about five hours. The spacecraft were placed in solar orbits that approached to within 0.3 AU of the Sun. The photometers of HELIOS 1 viewed to the south of the ecliptic plane, HELIOS 2 to the north. These photometers were first shown to be sufficiently sensitive to enable them to detect variations in density from coronal mass ejections by Richter *et al.* (1982). Although most of the bright transient events observed by the HELIOS photometers are mass ejections, elongated features that corotate with the Sun are also observed. Mass ejections are distinguished by their apparent outward motion that is primarily symmetrical to the east of the Sun as well as to the west. Corotating structures, on the other hand, can be observed as they move from east to west with time over many days.

The image processing system we have developed has been demonstrated by construction of several image sequences in video format of the interplanetary medium during mass ejection events. These data and additional data sets have been used to trace the time history of a variety of density enhancements. These programs have been transferred to different computer systems, creating the capability to carry out HELIOS data analysis at various laboratories. The ability to transfer this analysis to other locations has also become important as others view and make use of the data to determine the three-dimensional shapes of heliospheric structures. This capability will be especially important as we attempt to convert some of our enhanced data analysis techniques for use in forecasting analysis using the SMEI data set. The visualization programs we have developed, still crude but with clear potential, can be applied to many other data sets.

II.B.1. The HELIOS Photometer Data Set – CMEs

A major achievement of past research at UCSD has been the measurement of interplanetary masses and speeds of CMEs observed with coronagraphs, by interplanetary scintillation techniques and *in situ* spacecraft measurements. The combination of these data allow spatial configurations to be determined for each coronal mass ejection studied (Jackson, 1985a; Jackson *et al.*, 1985; and Jackson and Leinert, 1985; as reviewed in Jackson, 1985b). The 2-D imaging technique that by the displays HELIOS data has been developed here. Figure 2 shows an example of a set of contour plot images obtained following a solar mass ejection on January 2-6, 1979. Nearly 160 CMEs observed

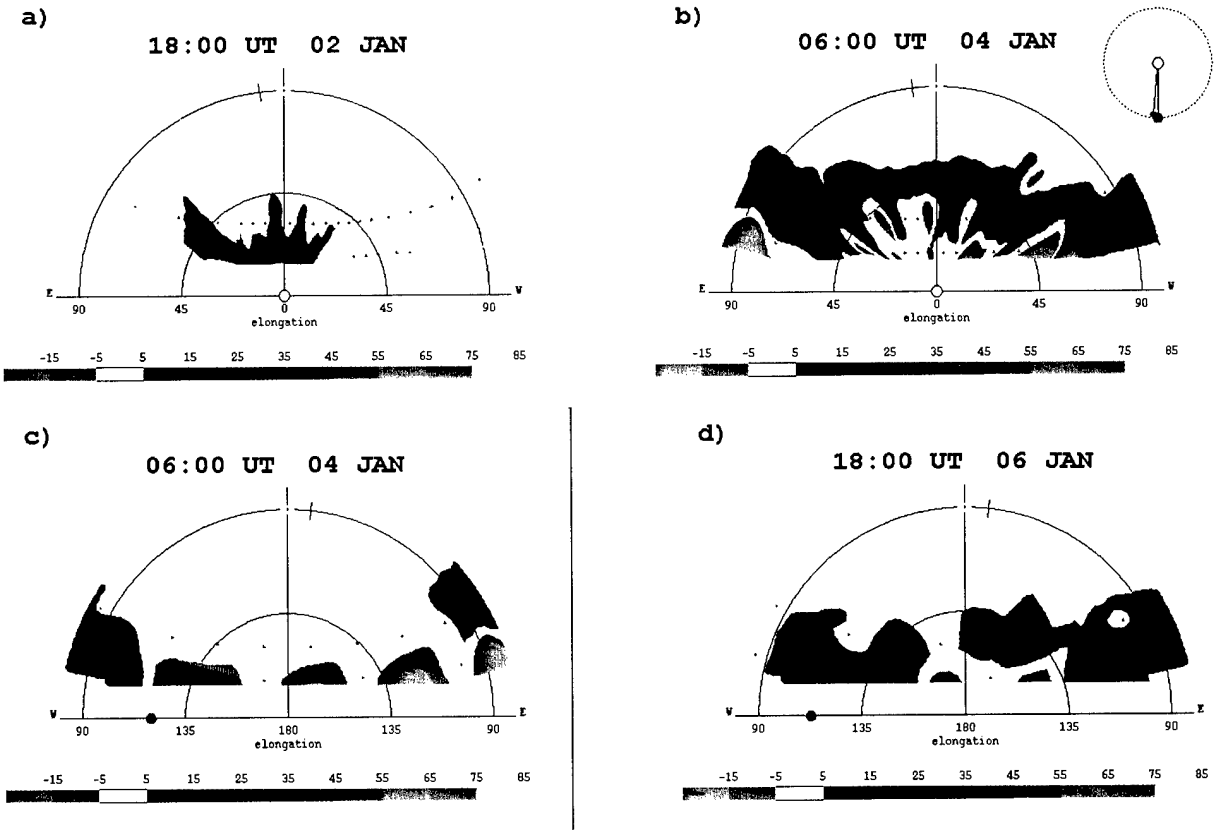

Fig. 2. Heliospheric images derived from the photometers on board the HELIOS 2 spacecraft when HELIOS 2 was 0.94 AU from the Sun. A CME is the primary structure imaged from 2 to 6 January 1978. The CME is observed to begin outward motion near the Sun and then move past the spacecraft. A diagram in the upper right of the figure indicates the position of the Earth, Sun and HELIOS 2. Electron column density is contoured in levels of 10^{14} cm^{-2}. **a)** and **b)** The Sun is at the origin with the horizontal axis representing the ecliptic plane. Radial distance from the origin represents solar elongation (as labeled on the horizontal axis). **c)** and **d)** As in **(a)** and **(b)** but with the anti-solar direction at the origin. The Earth position is marked as a blue dot between west 90° and 135°. Chronological sequences of these images reveal the dynamics of the ejection events observed. A video sequence from images of another CME (on May 24, 1979) is available on the web at: **http://casswww.ucsd.edu/solar/misc/heliosv.html**

HELIOS photometers have been imaged in this manner. We show this CME because it was observed when HELIOS 2 was almost 1.0 AU from the Sun and very near Earth. Additional information about this CME can be found in other studies (Burlaga *et al.*, 1981). The measurement of this CME by the HELIOS photometers essentially proves that heliospheric signals are sufficient for SMEI to be able to observe CMEs from Earth orbit.

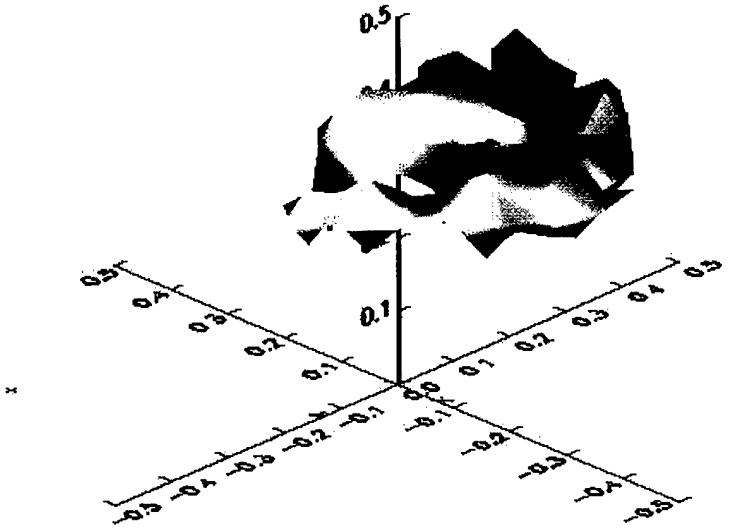

Fig. 3. Three dimensional density plot of the deconvolved 24 May 1979 CME as derived from SOLWIND coronagraph and HELIOS photometer data. The perspective view is from 30° above the ecliptic plane and 135° to the east of the Sun-Earth line. Distances on the axes are in AU. The contoured surface is a density level of 50 electrons cm^{-3} or greater.

The masses obtained from these observations indicate that indeed the material of a mass ejection in the lower corona moves coherently outward into the interplanetary medium. In HELIOS photometer data it is possible to sample the brightness of any given ejection over a far greater range of heights at one time than does a coronagraph. Individual mass ejections appear to have approximately three times as much mass in the photometer data as in older coronagraph observations (Webb *et al.*, 1995). By measuring the outward motion of an ejection, the total extent of mass flow past the 16° latitudinal photometer can be found and then checked by the second 31° photometer (*e.g.*, see Jackson, 1985b). The HELIOS data show that, not only do coronal mass ejections supply significant mass to the interplanetary medium, but that the mass flow extends over times that can be significantly longer than one day. That CMEs contain outflowing mass over long time periods has recently been confirmed by LASCO studies (e.g., Howard et al., 1997; Vourlidas et al., 2000).

The data from the HELIOS spacecraft photometers and the SOLWIND coronagraph have been used to reconstruct the three-dimensional shapes of coronal mass ejections in the interplanetary medium through computer assisted tomography (CAT) techniques (Jackson *et al.*, 1988; Jackson, 1989; Jackson and Froehling, 1995). These results were also described in Jackson and Hick (1994). The May 24 CME CAT reconstruction confirms the general shape of the most dense portion of this mass ejection as a shell-like feature, and confirms that this dense CME material was moving outward at speeds of ~1000 km s^{-1} at distances of 0.4 AU from the Sun. Figure 3 depicts these data (for the 24 May 1979 CME) at 09:21 UT 25 May. The HELIOS photometer data sets were made available on optical disk through NSSDC in 1989. Since then we have displayed all of the 90° photometer data for the HELIOS 1 and 2 spacecraft. From this complete data set from HELIOS 1 and 2, we selected all of the significant bright transient events (~300) for further study. This list of events has been published (Jackson *et al.*, 1994) and distributed to the community.

Using this list we published a preliminary study of the solar cycle variation of these data (Webb and Jackson, 1993) that was subsequently included with other CME data by Webb and Howard (1994) to show that CMEs are more frequent during the maximum of the solar activity cycle. Using this list Crooker *et al.* (1993) have developed a model where CMEs are channeled through the heliospheric current sheet and, thus, CMEs in their study are generally associated with the high density corotating regions. These analyses and the availability of the photometer data have lead to a variety of other studies, such as reported in papers by Webb *et al.* (1993a; b) and Jackson *et al.* (1993). Webb and Jackson (1992), Jackson and Webb (1994), Webb *et al.* (1995) and Webb and Jackson (1996) have continued analysis of the 90° events using the complete data set. They determine the solar cycle variation of the CMEs and compare the CMEs with the *in situ* plasma and interplanetary magnetic field present at the HELIOS spacecraft. SOLWIND and SMM coronagraph observations are compared in Webb *et al.* (1995). These comparisons show that CMEs measured in the heliosphere are more massive than when they are measured by a coronagraph in the lower corona.

II.B.2. The HELIOS Photometer Data Set – CRSs

Persistent elongated structures near the solar surface (streamers) that rotate with the Sun and extend outward from it are the most prominent coronal structures observed at the time of an eclipse. In the solar wind, dense regions that re-appear on consecutive solar rotations are also observed. The HELIOS observations have been used to measure the extent of these features (Jackson, 1991a). A portion of this study reported in Jackson *et al.* (1993) shows that about one-third of the CRSs are associated with sector boundaries observed in the solar wind.

A procedure has been developed at UCSD to use month-long stretches of photometer data to display heliospheric brightness in the form of synoptic charts (Hick *et al.*, 1990). These latitude-longitude contour plots give the heliospheric locations of persistent bright structures. This technique has most recently been transformed into a tomography program that has been used to reconstruct inner heliospheric densities and velocities using both IPS (Jackson *et al.*, 1997a; c) and HELIOS (Hick and Jackson, 1998; Jackson and Hick, 2000) data sets. For the first time these data show the latitudinal density structure of the heliosphere beyond the region of primary solar wind acceleration. Using this technique, it is possible to build up a contour map from observations toward the east of the Sun that sample the corotating structures before they reach the Earth. This technique demonstrates the possibility of being able to forecast the arrival of these features at the Earth. This corotating forecast capability is important because it has been shown that dense corotating regions are often associated with CMEs and geomagnetic storms (Crooker *et al.*, 1993), and that the low density coronal hole regions between these dense regions cause low-level magnetic storms due to their enhanced Alfven-wave flux (Tsurutani *et al.*, 1995). In addition, the dense corotating structures present in the solar wind can produce signals that obscure the observation and forecasting of CMEs.

In a preliminary report (Hick *et al.*, 1992) we compared these synoptic maps with IPS velocity maps (Rickett and Coles, 1991), K-coronameter maps (Fisher and Sime, 1984) and magnetic field maps (Hoeksema *et al.*, 1983). The HELIOS observations clearly show the organized heliographic equatorial enhancement of density at solar minimum and a depletion of the density over the solar poles. As solar maximum approaches, the enhanced density increases in latitude until at the time of maximum the whole of the Sun is surrounded by dense solar wind. This effect had been concluded from circumstantial evidence nearer the solar surface by others, but has

never before been as directly observed above the primary region of solar wind acceleration (where the HELIOS photometers are sensitive).

These observations above the acceleration region of the solar wind allow a direct comparison of the solar wind density variations with solar wind speed from IPS velocity data. The combined density observations (from HELIOS) and velocity measurements (from IPS) have allowed us to investigate variations of mass, momentum and energy flux in the solar wind with heliographic latitude and solar wind speed. Hick and Jackson (1994) in a preliminary analysis show that the momentum flux (mV^2) [and not mass flux (mV) or energy flux (mV^3)] is the same for the high latitude, fast solar wind and low latitude, slow solar wind. The implication of conservation of momentum flux poses a valuable constraint on solar wind modeling. In particular this implies that the total energy input to the solar wind (other than associated with CMEs) is constant over longitude and latitude and not enhanced significantly by the strong solar magnetic field near the solar surface above the regions of high solar activity. Leinert and Jackson (1998) have taken this concept one step farther and have derived the solar wind flux over solar cycle using this assumption and measurements from the HELIOS photometers and UCSD velocity IPS measurements.

II.C. IPS Observations

An enhancement to the north of the Sun on 29 April 1979 observed by the Cambridge IPS array had previously been identified by Hewish and Bravo (1986). The enhancement is located in the correct place expected for the mass ejection observed earlier by the HELIOS and SOLWIND spacecraft observations. Masses derived using Thomson scattering and IPS observations agree to within a factor of two of each other (Jackson, 1991b). Considering the errors involved and the assumptions made to arrive at these masses, the two techniques agree fairly well. It is somewhat disturbing that the IPS technique does not register this event as one of the most significant observed, since the Thomson scattering measurements do. This is one of the few events which Hewish and Bravo (1986) and others agree should be attributed to a CME.

IPS intensity observations from May 1990 until September 1994 from a single telescope array in Cambridge, England are available at UCSD. Velocity IPS observations have been available in a regular way continuously since about 1985. Two imaging display techniques have been developed at UCSD to determine the location of IPS structures in the heliosphere and these currently operate on the computer system in our laboratory. The two techniques display IPS observations as either daily "images" or synoptic maps. Daily images present the data as observed from Earth over the course of a day. Large regions of higher (and lower) than normal scintillation level can be viewed propagating outward through the heliosphere from one day to the next on these images. The images are currently presented in two formats as either position angle-elongation or Hammer-Aitoff projections. Figures 4a and 4b give examples of these image plots and are analogous to the images from the HELIOS photometers presented in Figures 2a - 2d.

The synoptic map technique allows a summary of daily data from present and past daily observations. Synoptic maps present an average of daily observations that can be used to enhance those structures that corotate with the Sun. This technique runs into difficulty when there is a predominance of transient events present in the heliosphere. Carrington synoptic maps of velocity and scintillation level are one of the techniques used to display IPS observations. Using the point-P analysis technique, it becomes possible to relate each observation to a given solar latitude and longitude. Scintillation level data from the Cambridge scintillation array analyzed in this manner show that the solar polar regions generally do not scintillate very strongly compared to regions near

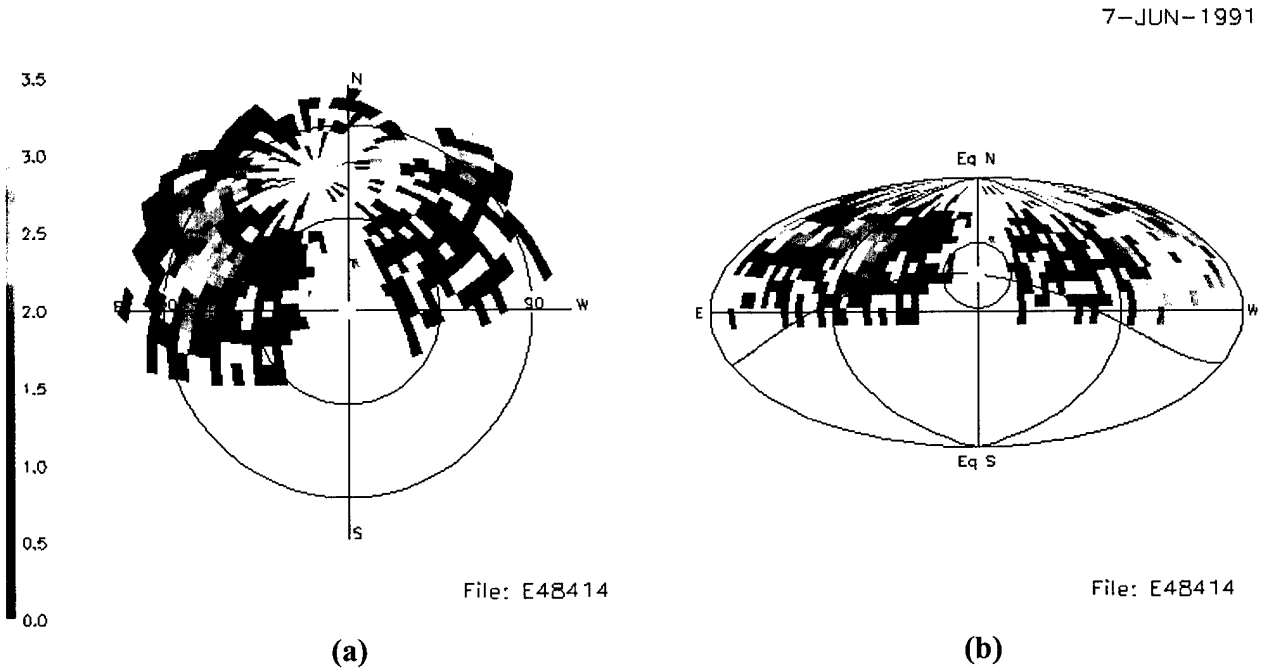

Fig. 4. Daily IPS intensity maps obtained on 7 June 1991. An interplanetary disturbance is observed moving outward from the Sun to the solar northeast. **(a)** Position Angle-Elongation plots of the IPS data. The Sun is centered in the image with elongation angles represented by equal linear distances from the Sun. Northeast is to the upper left on the plot. **(b)** A Hammer-Aitoff projection of the same data. The curved line through the center of the plot represents the ecliptic plane. West is left, east is right.

the solar equator. Hick *et al.* (1995a; b; c) have determined that solar active regions generally bright in X-rays, and not the current sheet, are usually the mapped solar surface locations of corotating regions observed to scintillate strongly in the Cambridge IPS observations. This was somewhat of a surprise, since the near-solar white light observations have usually been used to conclude that the region of the solar wind above the heliospheric current sheet is the most dense.

Both daily and synoptic map IPS displays are highly sensitive to the dense structures present in the solar wind along the line of sight. In order to answer criticisms of the point-P technique, which does not take into account this line of sight weighting, we developed a line of sight modeling technique which allows us to automatically take into account the line of sight variations in the observed data. This tomographic analysis (Jackson *et al.*, 1998; Jackson and Hick, 2000) least squares fits observational data to a simple heliospheric model giving the best fit possible including line of sight weighting variations (Figure 5).

In current analyses these tomographic heliospheric representations show essentially the same thing as the point-P analysis with respect to the position of dense structures. The dense structures present in the IPS data are often present above solar active regions and seldom fall on the heliospheric current sheet. The velocity IPS data analyzed using a similar tomographic technique (Kojima *et al.*, 1997) shows that these regions also have very slow solar wind velocity.

II.D. Additional Synoptic Observations

Both the HELIOS photometer observation and IPS measurements give information about the solar wind above its primary acceleration region. Imbedded in this quiet solar wind are dense, slow solar wind regions that can be observed as corotating structures (CRSs) in the interplanetary medium. In our attempts to study these regions in IPS and HELIOS data, we have expanded the study of the HELIOS photometer observations to solar surface and present-day measurements of these structures. During solar minimum conditions (for instance, 1994-1996) these solar wind structures dominate and may be responsible for more solar-terrestrial interactive effects than CMEs.

To study the above data sets we have mapped each in the form of a Carrington synoptic map format similar to those presented in the examples in Figure 6. Data sets presented in this way (in terms of solar latitude and longitude) for one or a combination of solar rotations allow the ready comparison of stable solar features in two dimensions. This type display enhances the ability to determine features associated with the Sun which corotate; presentation of consecutive rotations show those features which remain present from one rotation to the next.

Fig. 5. View of the corotating component of the plasma density in the inner heliosphere (out to 1.5 AU) derived by tomographic reconstruction from IPS intensity level data (Cambridge, UK) and IPS velocity data (Nagoya, Japan) for Carrington rotation 1884 (June 23 to July 20, 1994). The density is normalized by the removal of an r^{-2} distance dependence. The Sun is at the center; the Earth is marked in blue in its orbit around the Sun. The view is from 15° above the plane of the solar equator. The scintillation intensity level is calibrated in terms of density by comparison with IMP spacecraft densities at Earth. Clearly seen is the Archimedean spiral structure of the solar wind (as presented in Jackson *et al.*, 1998). An animated version of these data is available on the Web at: **http://casswww.ucsd.edu/solar /tomography /slow stel 1884.html**

III. Research Completed Under This Contract

During the first year of this contract the Air Force Space Test Program (STP) manifested SMEI on the Coriolis Mission along with a Navy spaceborne radar experiment named WINDSAT. The launch date for the Coriolis Mission is set for later in 2002 from Vandenburg AFB in California. The spacecraft will be placed in a terminator, polar, Sun-synchronous orbit. In the second year of this contract in the spring of 1999 Spectrum Astro Inc., was chosen to build the Coriolis bus.

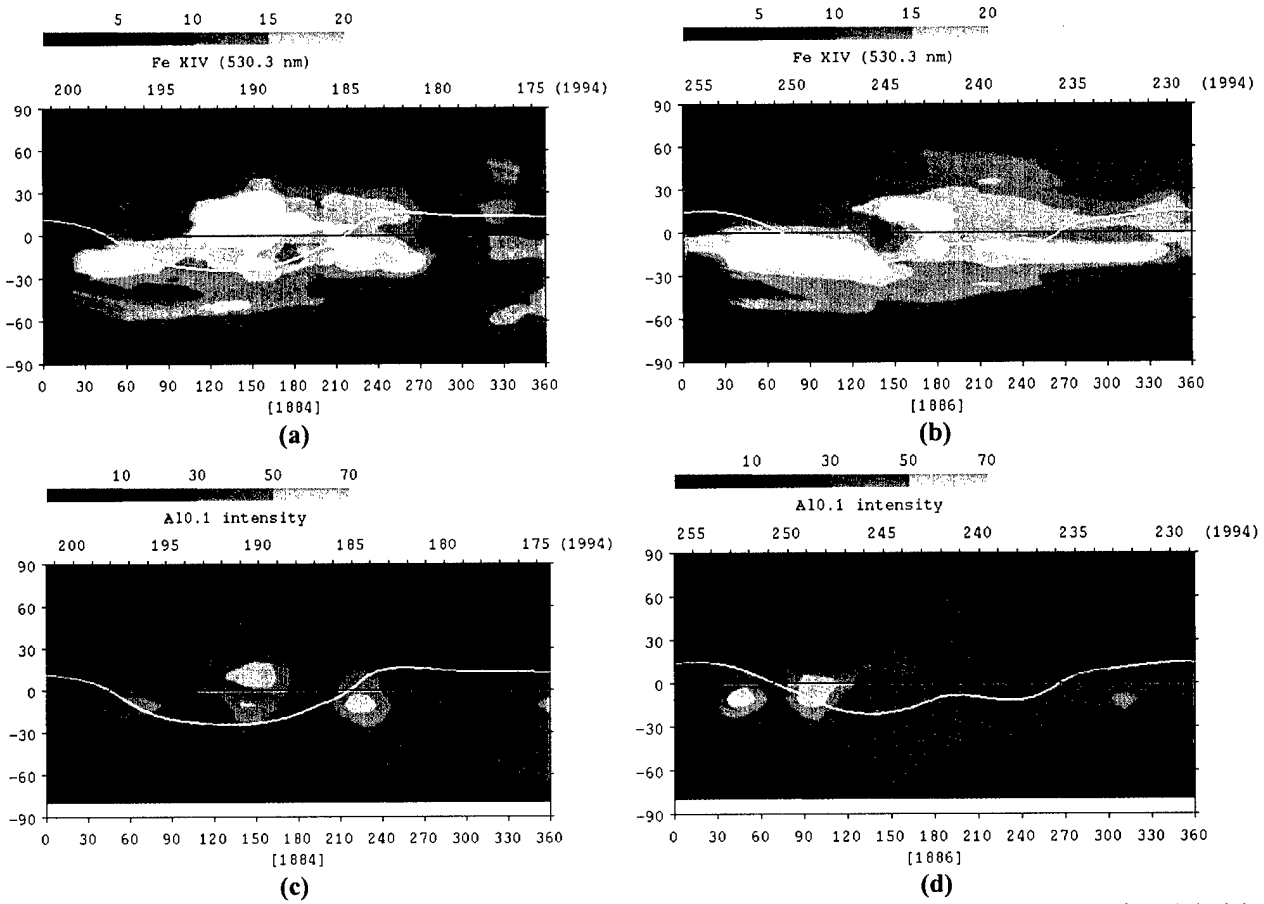

Fig. 6. Carrington synoptic map presentations of quiet Sun structure for rotation 1884 and 1886. **(a), (b)** Sacramento Peak Observatory coronagraph data from Fe XIV limb scans at 1.15Rs. **(c), (d)** YOHKOH SXT central limb data (assumed at a height of 1.15 R_S degraded to a 10°×10° resolution.

Over the three years of this contract we completed 32 research articles, gave 59 presentations and continued research on several aspects of the solar-terrestrial connection related to CMEs and the SMEI data analysis. We have provided the first images of the three-dimensional heliosphere in real time using interplanetary scintillation (IPS) data, and have analyzed HELIOS photometer data using these same techniques. Having made available the extensive *in situ* data set from the HELIOS spacecraft to be used by others in comparative studies with the photometer data, we have also used this data set to study CMEs. We have also begun to use the extensive data set from the LASCO coronagraphs in order to make fundamental new solar wind studies.

Both interplanetary scintillation observations and the HELIOS photometer data set have been employed to map various aspects of the solar wind using a variety of techniques. In particular, we developed a tomographic analysis technique to determine the three-dimensional structure of the quiet solar wind into which the CMEs emerge and refined this technique so that it can be used to map transient structures as well as corotating ones.

We also began a real-time analysis of IPS velocity observations with our Japanese colleagues at STELab which operates continuously and is used to forecast solar wind conditions at Earth. This uses a technique similar to one that will be used with SMEI data when it becomes available. Specific progress over the contract period is described below.

III.A. Heliospheric Imagers

III.A.1. The Solar Mass Ejection Imager (SMEI)

Although the construction and tests of the SMEI instrument are funded at UCSD by another contract, the data analysis schemes designed for SMEI must necessarily conform to the SMEI specifications. For this reason we mention the current status of the SMEI instrument development in the following paragraphs. The SMEI instrument consists of three camera subsystems, each containing a wide-angle aperture carefully baffled to minimize stray light, and an optical system feeding a CCD camera. The current prototype includes a test baffle, a CCD camera and a wide-angle optical system. Construction and work to refine the SMEI design has continued with a science team from the groups at UCSD and the Air Force Research Laboratory, Hanscom as well as the University of Birmingham, UK.

The optimum orbital deployment for the instrument requires a stabilized, zenith-nadir pointing spacecraft in an orbit at ~850 km. This altitude is a compromise between the need to be above as much of the Earth atmosphere and auroral glow as possible and the need for ease in launching a spacecraft with the greatest payload weight. For instance, instrument design requirements permit a launch into a circular equatorial orbit by a PEGASUS rocket.

Each of SMEI's three cameras covers a different 3°×60° field of view such that together they view a slice of sky 3° wide, spanning an arc ~180° across the sky. Although the exact operation close to the Sun will be determined on orbit, viewing within about 18° of the Sun and the images containing the moon and a few pixels containing bright planets will generally be excluded. The detector look directions, as defined by the 180°-arc field of view plane, are oriented with a horizontal line through this plane roughly perpendicular to the spacecraft orbital velocity vector. Thus, the cameras, rigidly mounted to the spacecraft, sweep out nearly the entire sky once every 100-minute orbit.

The accommodation of SMEI on the Coriolis mission has not been a simple one for UCSD. The Coriolis Mission, which includes both SMEI and the Navy's WINDSAT spaceborne radar antenna experiment has required significant UCSD research and development in order to certify that SMEI will work in conjunction with the WINDSAT radar antenna. The WINDSAT antenna occupies the location on the spacecraft bus (zenith side) for which SMEI was originally designed.

Originally the baffle system was designed to look upward in approximately the zenith direction and more than 90° away from any portion of the spacecraft bus. However, the Coriolis Mission has required relocation of the SMEI cameras to the side of the spacecraft bus, and to view approximately 25° from the horizontal with the WINDSAT antenna and some portions of the spacecraft bus necessarily close to the SMEI field of view. Thus, the baffle and optical system must now perform extremely well to remove stray light in order to accomplish this. The prototype baffle system, blackened by the proprietary Martin Black process in May and June 1998, was not as black as the Martin Lockheed group originally intended. This caused an approximate order of magnitude decreased stray light rejection capability for the baffle and considerable discussion among the SMEI collaborators. However, tests at UCSD show the stray light rejection can still be handled adequately by a carefully designed optical system. Design and testing continued at UCSD on these items and were incorporated into the flight camera design. In addition, several tests on a test panel provided by Martin Lockheed in the spring of 1999 during the blackening of yet another SMEI prototype baffle have shown that they may have recovered their original blackening process.

The optics designs for SMEI were finalized and the vendor chosen by UCSD to make the diamond-turned mirrors is Hyperfine of Boulder, Colorado. Hyperfine successfully produced these mirror optics. The flight cameras and optics together were tested and they were subsequently confirmed to operate to the designed 0.1% photometric performance specification for small motions of point light sources in the camera field of view. Further tests and certification of the large-scale 0.1% photometric specification must wait for spacecraft launch. Current tests are limited by the stability of ground-based light sources and the inability of cooling the flight CCDs until the spacecraft is in orbit.

The SMEI Critical Design Review (CDR) was held in August 1999, and the instrument passed this review satisfactorily. The instrument was completed and delivered to Spectrum Astro in April 2001.

III.A.2. Other Imager Designs

SMEI has been designed for use in Earth orbit and is currently the best design we know for operation near Earth and where the Moon and stray light from spacecraft bus appendages have the potential to overwhelm the faint brightness signal from heliospheric electrons. However, in deep space a lightweight version of SMEI on a dedicated instrument bus could view the whole sky over a hemisphere or more in a single image. One of us (A. Buffington) has championed this type imager and presented the studies of this type of design in several papers (Buffington *et al.*, 1996; 1998, Buffington, 1998; 2000). Though not funded by this contract, we continued to develop this instrument concept in preliminary form for several NASA-proposed spacecraft including STEREO, Solar Probe and Solar Polar Sail. UCSD submitted a proposal to the STEREO announcement of opportunity for construction of the Heliospheric Imager (H.I.) during the second report period of this project. This UCSD proposal was unsuccessful. A second proposal using a similar instrument design was submitted to NASA during the last year of this project for inclusion on Solar Probe. The results of the Solar Probe review have not yet been announced.

III.B. Research on Coronal Mass Ejections (CMEs)

Under this grant we performed several CME studies. Some of these will be incorporated into the forecasting and research analyses and will utilize that SMEI data when it becomes available. Part of this work effort involved studies of the environment, especially the magnetic field structure, of the sites of origin of CMEs, how they develop in the corona, and what their signatures are in and how they propagate through the interplanetary medium. We studied the surface manifestations of CMEs and how they relate to the ensuing disturbance in the interplanetary medium. We also studied what the most reliable indicators are on and near the solar surface of the launch of CMEs and what these tell us about how geoeffective a given CME will be. We studied what parameters of CMEs observed both near the Sun and in the interplanetary medium cause the largest geomagnetic storms.

III.B.1. HELIOS Photometer Studies

CME research is one of the most significant kinds of studies that resulted from the HELIOS photometer observations. In the past we have published many results using the HELIOS CME data. Under this grant we performed several follow-up studies using these data sets, including the determination of the signatures of geoeffective solar ejecta propagating through the interplanetary

medium, and which properties of such interplanetary CMEs, such as mass, momentum, speed and total pressure, are best correlated with geomagnetic storms. We published revised papers (Webb *et al.*, 1997a, b) on the results of studying HELIOS CMEs that were aimed at the Earth.

In another study we determined the speeds in the inner heliosphere for ~130 of the CMEs in the list of 160 CMEs observed by the HELIOS photometers published earlier (Jackson *et al.*, 1994) under the previous contract. For these events we are revising a manuscript to be submitted for publication that details the speeds of CMEs in the solar wind and compares these speeds to other published observations (Jackson and Webb, 2001).

III.B.2. Sources and Geoeffectiveness of SOHO Halo CMEs

Under this contract we studied the characteristics of the source regions of CMEs and what the surface manifestations and the development of the CME itself can tell us about the geoeffectiveness of a given CME. Of most interest is what the characteristics are of those CMEs that result in the largest geomagnetic storms. These studies were led by Co-I D. Webb.

One of the major discoveries with the SOHO LASCO coronagraph data has been the imaging of enhanced outward-flowing excess mass surrounding most or all of the occulted solar disk during a CME. These so-called "halo" events indicate that the CME is aligned along the Sun-Earth axis and, therefore, is aimed either in the direction of Earth (i.e., the SOHO spacecraft is at the L1 point in front of Earth) or in the opposite direction away from Earth. When halo CMEs are accompanied by observable surface activity, it is likely that the event erupted from the "frontside" of the Sun. If the surface activity is within ~0.5 Rs of Sun center and it is likely aimed toward the Earth and will be geoeffective (e.g., Webb *et al.*, 2000a, b). We have studied both the nature of this associated surface activity (Webb *et al.*, 1998a, 2000a, b; Hudson *et al.*, 1998) and the effects of the halo events at Earth (Webb *et al.*, 1997d; Webb *et al.*, 1998c, d; Webb *et al.*, 2000a, b; Burlaga *et al.*, 2001). In the earlier studies we found that, just after solar minimum (1996-1997), halo CMEs were typically associated with small, long duration X-ray arcade flares, EUV waves, transient coronal dimming regions, and erupting filaments, within about 0.5 solar radius of Sun center.

However, the activity was highly variable from event to event and, in the case of the January 1997 halo CME, the significant geomagnetic effects would not have been forecast if the halo CME had not first been observed by LASCO (Webb *et al.*, 1998a, 2000a). Except for the newly discovered EUV waves, all of these types of activity have been well associated with CMEs in the past. At the Earth the LASCO halo events associated with frontside activity were always followed (in 6 out of 6 cases) 3-5 days later by an interplanetary shock, a magnetic cloud and a moderate-level (Dst > -50 nT) or greater geomagnetic storm. This is despite the fact that these events appeared to be relatively weaker as expected for near-solar minimum activity.

Recently, we have extended this study to include all halo CMEs observed by LASCO through 1999 (Webb, 2000c, d). We concluded the following: a) Halo CMEs are important for space weather research because they permit sampling of the structure of a CME along its axis, and they can improve our forecasting of Space Weather phenomena. b) Some important characteristics of halo CMEs are that ~11% of all CMEs appear as halos and 4% are full (360 deg.) halos, and the average halo CME speed is 740 km/s., much greater than the average for all CMEs. These results suggest that CMEs observed as halos by LASCO are generally denser and faster, and probably more energetic, than the average CME. c) The kinds of solar surface activity associated with the halos is similar to and extends previous results. This activity includes flares, coronal (EUV) waves, dimmings, long-enduring arcades, and erupting filaments. The average distance of the source from

Sun Center is ~30°, and most halo-related activity is within $0.5R_S$ of Sun Center. Thus, the surface activity is typically offset from the CME axis.

From 1996 through 1998 we searched for associated activity at 1 AU 2-5 days after the halo CME onset by examining Wind and ACE spacecraft solar wind data and geomagnetic indices. In about 2/3 of the cases, we found that IP shocks, magnetic clouds/flux ropes, counterstreaming electrons and anomalous or high density plasma, indicative of closed field lines and filaments, respectively, arrived at 1 AU with an average travel time from solar onset to 1 AU of 3.6 days. We also found that the halo CMEs were typically associated with at least moderate-level geomagnetic storms 3-5 days later.

More recently, an extension of this study through 1999 suggests that the geoeffectiveness of halo CMEs falls off toward solar maximum. This might arise because of the increasing complexity of the solar magnetic field, including the higher inclination of the current sheet. Thus, despite the increasing number of CMEs toward maximum, the fraction entering the ecliptic is reduced and their inclinations are not as favorable for interaction with Earth. Webb participated in the international Space Weather Month study of September-October 1999, which culminated in a workshop at the S-RAMP meeting in Sapporo, Japan (Webb, 2000e). During this period two great storms occurred which were driven by the interaction of halo CMEs with corotating solar iend structures which enhanced the southward fields.

Thus, it appears that shocks and magnetic clouds, possibly arising from filament-related flux ropes, and other evidence of closed field lines, appear to be characteristic of at least the larger CMEs. These features are most notable in this data set because we sample the CME material nose-on at 1 AU. Such flux ropes may be associated with depletions of the coronal material at their feet. The importance of such observational studies to understanding CMEs and developing forecasting techniques for future instruments like SMEI and STEREO is clear.

III.B.3. The Magnetic Field Structure of CMEs

Under this contract we also studied the magnetic topologies of individual CMEs, especially of their source regions and how they erupt and develop into interplanetary disturbances. Earlier we published a paper providing strong evidence that the source regions of at least many CMEs involves complex magnetic topologies, especially quadrupolar structures (Webb *et al.*, 1997c). One aspect is that the span of typical CMEs can cross 2 or more neutral lines at the surface, suggesting that multiple closed-field arcades lay underneath the CME before its eruption. CMEs can also arise over convoluted neutral lines, such as those having a "switchback", or hairpin appearance, as has also been noted by McAllister and colleagues. This study was done before the launch of SOHO; observations with LASCO of multiple arcades near the surface (C1 coronagraph) underlying a single helmet streamer further out (C2 and C3) and multiple arcades evolving into a single central CME now support our idea.

We are working on a paper wherein two Yohkoh X-ray events exhibiting quadrupolar structure are compared with white light CMEs and with the multipolar CME model of Antiochos *et al.* (1999). The preliminary results were presented during earlier by Webb *et al.* (1998c). We examined the Yohkoh and EIT data for other multiple arcade coronal events that are associated with CMEs to see how common they are, and, *e.g.*, whether complex magnetic structures are a necessary condition for the occurrence of a CME.

With additional support from another grant, we also performed two preliminary studies of the observational evidence for and the characteristics of the disconnection of magnetic field lines

involved with CMEs. The first study was of the characteristics of disconnection events observed with the SMM coronagraph from 1984-1989 (Webb and Burkepile, 1998). About 10% of all SMM CMEs exhibited such concave-outward structures. These events often involved the blowout of a pre-existing streamer and in half of them a narrow, bright ray suggesting a current sheet appeared ~12 hr. later. The disconnection structures tended to be half as wide and half as slow as their associated CMEs.

Recently, we studied the late, raylike structures to test how their characteristics compared to the Lin and Forbes (2000) model of flux ropes and current sheets. About half (25) of the SMM disconnection structures had new, transient, late rays. We found that the rays had average widths of 1.5°, and the axes of the CME and its associated ray were offset by an average of ~9°. Most of the rays were coaxial with the earlier concave-outward structure, and non-radial and directed toward the solar equator. The lifetimes of the rays averaged ~8 hr. If we assume that the rays extended from just above the surface to the back of the concave-outward structure in each event, then the lengths of the rays averaged 3.25 to >11.3 R_S. In comparison with the Lin and Forbes model, the widths of the rays were consistent with narrow, dense current sheets. Their lengths were roughly consistent with the model, but the height-time evolution of the bases and tops of the structures do not agree with the model. Much of this work was done under this contract, although the results were presented after its completion (Webb et al., 2001). We are writing a paper on the results, and also plan on analyzing SOHO-era data for such rays.

The LASCO data themselves have been studied by Webb *et al.* (1998b) and St. Cyr *et al.* (2000) who found that LASCO detected concave-out structures much more frequently than with previous coronagraphs. During 1997 such structures were found within nearly half of all CMEs. However, LASCO is also seeing complete circular structures within many CMEs, some of which have been modeled as flux ropes (*e.g.*, Chen *et al.*, 1997; 2000). Reconnection/disconnection may or may not be important in the formation of such events.

III.C. Tomographic Analysis and Program Improvements

The perspective views of the heliosphere formed by solar rotation and outward solar wind flow are used in our tomographic technique to determine three-dimensional heliospheric structure in an iterative process. The technique currently least-squares fits the available data. The three-dimensional model from this analysis can incorporate both the IPS scintillation level enhancements (from Cambridge, England (1991-1994), Ooty, India and Nagoya, Japan) and IPS velocities from UCSD (1965-1985) and Nagoya, Japan (1985-present).

These studies have resulted in a series of papers about the tomographic technique written jointly by the group in Toyokawa City and UCSD. In these papers (Jackson *et al.*, 1998); Kojima *et al.*, 1998; Asai *et al.*, 1998) the tomographic method (slightly different at the two laboratories) is described and preliminary comparisons with other data sets is made. Because the model is three-dimensional, we can form the synoptic map presentation at different heights and present the results in three-dimensions as in Figure 5. As expected, the structures mapped in density clearly show the Archimedean spiral structure present in the solar wind. Some of these structures show enhancement relative to the ambient plasma with height while others do not. These differences with height reflect both the model parameters which increase or decrease according to mass conservation within given latitude bands and the least squares fitting.

These data related to the location of spacecraft can be mapped as in-situ measurements of density and velocity observed at the spacecraft in order to determine the validity of the model and the accuracy of the observational fits. We are able through this technique to map the degree of scintillation level to density measured by spacecraft *in situ*. The velocities also are compared to *in situ* measurements and these correlate one-to-one with *in situ*-measured velocities.

III.C.1. HELIOS tomographic analyses

The tomographic technique has been used on Thomson-scattering white light data from the HELIOS photometers in a manner similar to the IPS analyses. These studies are shown to successfully map heliospheric structures and they appear to look much like those observed in the IPS tomography analyses. Preliminary papers by Hick and Jackson (1998) and Jackson and Hick (2000) describe the results of this technique. The results of the study of one month of HELIOS 1 and 2 data obtained by the spacecraft in 1997 are shown in Figure 7.

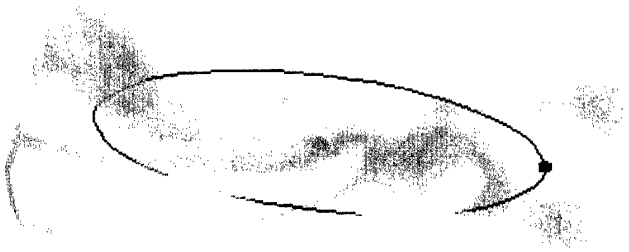

Fig. 7. View of the corotating component of the plasma density in the inner heliosphere (out to 1.5 AU) derived by tomographic reconstruction from HELIOS 1 and 2 photometer data and IPS velocity data from UCSD for Carrington rotation 1653 (March 21, 1977, to April 18, 1977). The density is normalized by the removal of an r^{-2} distance dependence. The Sun is at the center; the Earth is marked in blue in its orbit around the Sun. The view is from 15° above the plane of the solar equator. Clearly seen is the Archimedean spiral structure of the solar wind (as presented in Jackson and Hick 2000). An animated version of these data is available on the Web at: **http://casswww.ucsd.edu /solar/tomography/slow_helios_1653.html**

III.C.2. Heliospheric Densities from IPS Tomography

A comparison of YOHKOH and Sacramento Peak Fe XIV data on a rotation by rotation basis shows a great similarity of bright structures (active regions) with interplanetary scintillation (IPS) enhancements observed from 0.5 to 1.0 AU even though this correspondence is not observed in the magnetic field data extrapolations (Hick *et al.*, 1995a; b; c; 1999). These comparisons have indicated that solar active regions are major contributors of slow solar wind and that these regions add significant mass to the interplanetary medium. These regions (and not the heliospheric current sheet) dominate the IPS observations of the quiet solar wind at 1 AU. The regions of enhanced scintillation are generally regions of

denser solar wind (Jackson *et al.*, 1998). This distinction would go unnoticed except that previous understanding had indicated that solar active regions were closed magnetic structures with solar wind flowing around them.

Švestka *et al.*, (1997; 1998) and Hick *et al.* (1999) have used these analysis techniques to study outflows from active regions over many days and show that these outflows have significant variability. These researchers conclude that this variability is associated with the presence of activity in the form of CMEs and solar flaring from the active regions studied. It is uncertain from these studies if CMEs are the only way active regions can supply mass to the solar wind and the authors of these studies are divided on this issue pending further analysis of the data.

III.C.3. Time-Dependent Tomography

In order for SMEI to be to be ultimately successful, the data from SMEI will need to be analyzed using a tomographic technique that not only shows corotating structure, but also shows the dynamics of this structure as it moves outward towards Earth. Modifications of the Thomson-scattering tomographic technique now enable this type analysis. This not so simple modification of the computer programming technique has so far been termed 'time-dependent' tomography (Figure 8) because it allows temporal changes to be mapped in heliospheric structures. When short intervals

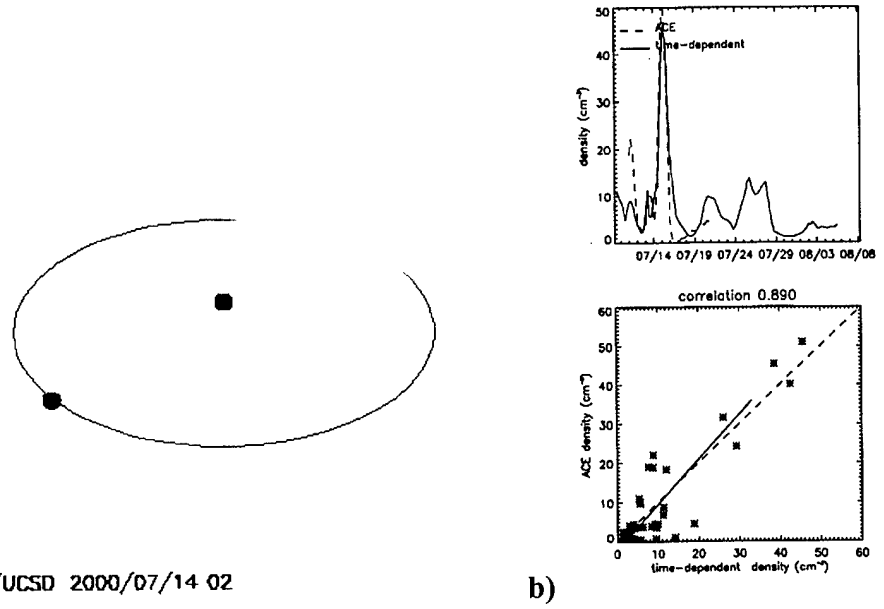

Fig. 8. a) Remote observer view of the heliosphere on July 14, 2000 from 30° above the ecliptic plane and 45° west of the Sun-Earth line. **b)** Time-series correlation during the event sequence.

of time are reconstructed in three dimensions this is akin to an analysis that derives its perspective views from the outward plasma flow alone. Current versions of this technique allow changes from 1 day to a half of a Carrington rotation to be used in the mapping.

The best results using this technique are expected from data sets with the least amounts of noise and with the most daily observations. While this technique has been demonstrated using Cambridge scintillation-level data and HELIOS photometer data using temporal intervals as short as one day, the best results from comparison with Earth *in situ* measurements using Cambridge IPS data appear to be analyses that map structures over about 4-day intervals. However, preliminary

comparisons of the Cambridge, England time dependent tomographic results with *in situ* observations at Earth are sufficiently better than those using a corotating assumption alone that we have felt justified in presenting the three-dimensional results (Jackson *et al.*, 1999a, b [Abstracts]) as accurate representations of heliospheric CME structures. The technique was used to successfully image the July 14 Bastille-Day CME and the time periods surrounding this event. Figure 8a shows the July 11 halo and a video at: **http://casswww.ucsd.edu/solar/tomography/fast_stel_1965.html** presents the whole of Carrington Rotation 1965 following this CME, and includes the July 14 halo CME. Figure 8b shows the correlation of *in situ* density with density determined by the time-dependent model for ±5 days of the Earth arrival of the July 14 CME. We are currently testing this technique in as many ways as we can in order to refine our tomographic programming techniques, and we have incorporated the use of this technique in our real-time analyses described in the next section.

III.D. Solar Wind Real-Time Observations

In order to test the higher-level forecast programs for SMEI that will be used to forecast the arrival of corotating structures and CMEs at Earth we have begun a real-time space weather program at UCSD. The Fortran programs that provide the tomographic result and the IDL images that are given by these analyses to provide Web images operate without human intervention once the data arrive at UCSD. These programs are run and continuously updated using Redhat LINUX 'Cron. Jobs' operated on a PC. The real-time analysis provides a daily map of solar wind structures around Earth (Figures 9a-d). The results of this analysis at Earth are checked hourly by comparison with measurements available from the ACE spacecraft operated from the L1 LaGrange point between Sun and Earth. These programs, which provide a daily comparison of the tomographic programming, show just how well real-time forecasts using current data sets work, and they show the way SMEI will be able to help in these forecasts in the future. The results of these real-time analyses are given at: **http://casswww.ucsd.edu/solar/forecast/index.html.**

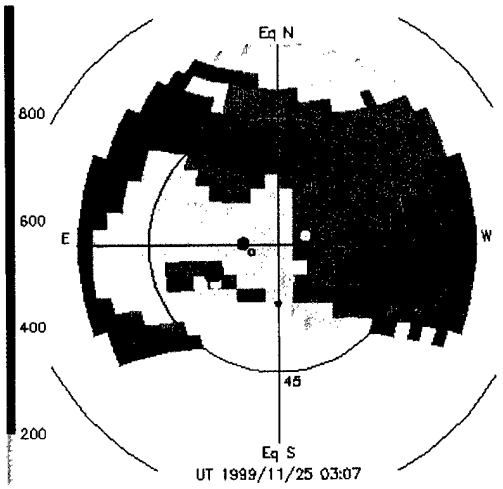

Fig. 9a. A recent sample sky sweep map showing the ambient solar wind velocities as observed from Earth with the IPS sources observed over the most recent 24-hour period superposed. The color of the source is the velocity observed for that source and the size of the source depicts the difference of the source from the nominal velocity at that location.

The interplanetary scintillation data set that is currently available is from the IPS array system located near Nagoya in the central region of Japan and operated from the Solar-Terrestrial Environment Laboratory (STEL) located in Toyokawa City. Following his stay as a visiting professor in the latter part of 1995, B. Jackson maintained his contact with this group and began a joint UCSD-STELab five-year collabora-tive agreement. The joint agreement began on December 15, 1997. The intent of the agreement is to provide collaborative exchange of ideas, personnel, current IPS data and ultimately SMEI data sets, and to make these data available in a forecast mode in both countries. The Nagoya data gives solar wind velocities from multi-site radio telescopes, which map the motion of the intensity-scintillation pattern across the

surface of the Earth.

Under the auspices of a Japanese Solar-Terrestrial Laboratory (STEL) - UCSD cooperative agreement, we have been able to obtain these velocity scintillation data in real-time. We were able to modify our HELIOS photometer data display programs to produce interplanetary scintillation daily maps (images) of the sky around Earth much as was done at NOAA in their attempts to forecast the arrival of heliospheric disturbances at Earth (Figure 9a). Only approximately 20 sources are tracked regularly each day, and so the data have limited usefulness in mapping discrete solar wind disturbances. Nevertheless, these data can be used to indicate the Earth approach of fast transient structures superposed on more quiescent solar wind structures.

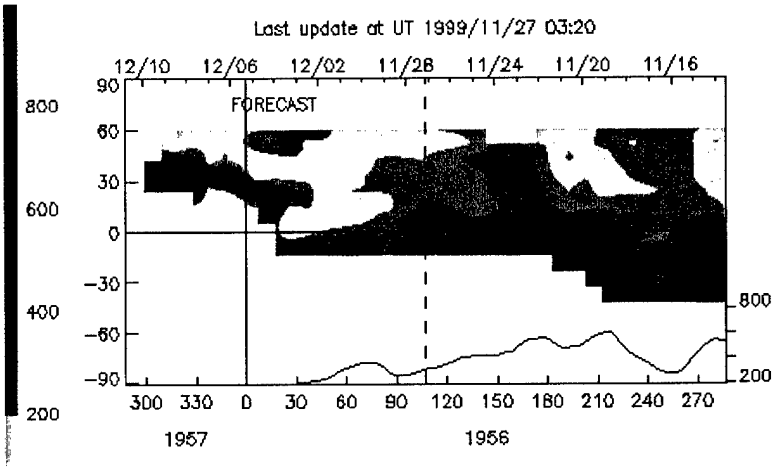

Fig. 9b. Carrington synoptic presentation of real-time solar wind velocity. The Earth is centered in the plot at the location of the dashed line. A trace of the velocity at Earth is shown below the map.

In real-time the three-dimensional velocity least-squares fit model is plotted in two dimensions (Figure 9b). The structures shown in Carrington coordinates at 1 AU give the best least squares fit to our 3-D tomographic model assuming corotation. The three-dimensional model from which the map is determined is also used to obtain a trace of the velocity at the heliospheric latitude, longitude and solar distance of Earth and this velocity is plotted below the Carrington Map. At this time in the solar cycle there are many high-speed structures present in or near the heliospheric equator. We suppose that these high-speed structures are primarily transient ones that persist long enough to be counted as enhancements in solar wind velocity at Earth. More definitive determinations of these structures may become possible using current time-dependent tomography techniques. We have modified our time dependent tomography technique to reconstruct temporal daily differences in structure and operate using velocity IPS data from STEL, Japan. To do this we have had to limit structure spatial resolution to 20° by 20° in heliographic latitude and longitude. The current velocity IPS tomographic analyses converge when we do this, but because the spatial resolution is limited to this

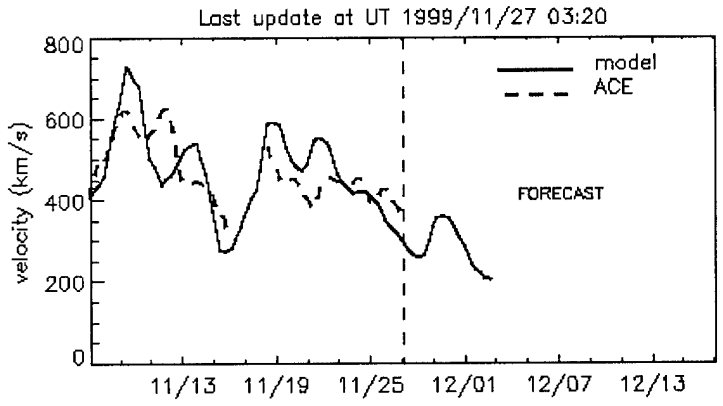

Fig. 9c. Time model presentation (time runs left to right) of IPS and ACE (in situ) velocity data. The model data is the same as plotted below the synoptic presentation in Figure 9b, and shows the least squares fit to corotating structure. In order that the ACE data compare in resolution with the IPS modeling it has been averaged to 18-hour intervals.

large extent it will allow reconstruction of only the largest heliospheric features.

In order to evaluate our different modeling techniques we compare them with *in situ* velocity measurements from ACE. Two time model presentations are given. In one we show our preferred model (currently corotating velocity using the UCSD reconstruction technique, Figure 9c), and in the second we show as many as three or four different models (Figure 9d sample) using different tomographic techniques such as the time-dependent technique. As the comparisons continue we expect some of these modeling techniques to survive while others will not.

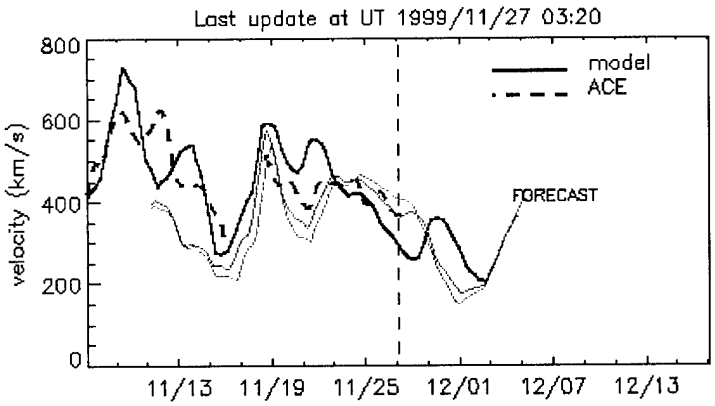

Fig. 9d. Model data comparison with ACE velocity data. Two versions of the time-dependent velocity model are shown for comparison with the "preferred" corotating one given in Figure 9c.

III.E. Recent Publications

The publications that have benefited from this grant or form the basis of research from it follow:

Research Articles:

Current research articles pertaining to the *present* grant include:

1. Kojima, M., K. Asai, B.V. Jackson, P.L. Hick, M. Tokumaru, H. Watanabe, and A. Yokobe, "Solar Wind Structure at 0.1-1 AU Reconstructed from IPS observations Using Tomography", in X.S. Feng, F.S. Wei, and M. Dryer (eds.), *Advances in Solar Connection with Transient Interplanetary Phenomena*, Proc. 3rd Symposium on Solar Transient Interplanetary Phenomena, October 14-18, 1996, Beijing, China, International Academic Publishers, Beijing, China, p.207 (1996) (6 pages). +

2. Jackson, B.V., P.L. Hick, M. Kojima and A. Yokobe, "Heliospheric tomography using interplanetary scintillation observations", *Physics and Chemistry of the Earth*, **22**, No. 5, 425 (1997) (10 pages). +

3. Jackson, B.V., A. Buffington, P.L. Hick, S.W. Kahler, G. Simnett and D.F. Webb, "The solar mass ejection imager", *Physics and Chemistry of the Earth*, **22**, No. 5, 441 (1997) (4 pages).

4. Švestka, Z., F. Farnik, H.S. Hudson and P. Hick, "Post-Flare Loops Embedded in a Hot Coronal Fan-like Structure", in A. Wilson (ed.), 31st ESTLAB Symposium: *Correlated Phenomena at*

the Sun, in the Heliosphere and in Geospace, ESA SP-415, ESTEC, Noordwijk, Netherlands, p. 139 (1997) (6 pages).

5. Webb, D.F., B.V. Jackson, and P. Hick, "Effects of CMEs on the heliosphere and geomagnetic storms using HELIOS data", in *Workshop on Solar Flares and Related Disturbances*, edited by E. Sagawa and M. Akioka, p. 276, Hiraiso Solar-Terrestrial Research Center, CRL, Isozaki, Japan, Oct. 1997.

6. Webb, D.F., B.V. Jackson, and P. Hick, "Effects of CMEs on the heliosphere and geomagnetic storms using HELIOS data", in *Solar-Terrestrial Predictions - V*, edited by G. Heckman *et al.*, p. 188, Hiraiso Solar-Terrestrial Research Center, CRL, Isozaki, Japan, Nov. 1997.

7. Webb, D.F., S.W. Kahler, P.S. McIntosh, and J.A. Klimchuk, "Large-scale structures and multiple neutral lines associated with CMEs", *J. Geophys. Res.*, **102**, 24,161, 1997.

8. Webb, D.F., E.W. Cliver, N. Gopalswamy, H.S. Hudson, and O.C. St. Cyr, "The solar origin of the January 1997 coronal mass ejection, magnetic cloud and geomagnetic storm", *Geophys. Res. Lett.*, **25**, 2469, 1998a.

9. Hudson, H.S., J.R. Lemen, O.C. St. Cyr, A.C. Sterling, and D.F. Webb, "X-ray coronal changes during halo CMEs", *Geophys. Res. Lett.*, **25**, 2481, 1998.

10. Webb, D.F., "CMEs and Prominences and Their Evolution Over the Solar Cycle", in *New Perspectives on Solar Prominences*, edited by D. Webb, D. Rust and B. Schmieder, ASP Conf. Ser. Vol. **150**, p. 463, BookCrafters, San Francisco, 1998.

11. Cliver, E.W. and Webb, D.F., "Disappearances of High-Latitude Filaments as Sources of High-Latitude CMEs", in *New Perspectives on Solar Prominences*, edited by D. Webb, D. Rust and B. Schmieder, ASP Conf. Ser. Vol. **150**, p. 479, BookCrafters, San Francisco, 1998.

12. Jackson, B.V., P.L. Hick, M. Kojima and A. Yokobe, "Heliospheric Tomography Using Interplanetary Scintillation Observations 1. Combined Nagoya and Cambridge data", *J. Geophys. Res.*, **103**, 12,049 (1998) (19 pages). +

13. Kojima, M., M. Tokumaru, H. Watanabe, A. Yokobe, K. Asai, Jackson, B.V., and P.L. Hick, "Heliospheric Tomography Using Interplanetary Scintillation Observations 2. Latitude and Heliocentric Distance Dependence of Solar Wind Structure at 0.1-1 AU", *J. Geophys. Res.*, **103**, 1981 (1998) (9 pages). +

14. Asai, K., M. Kojima, M. Tokumaru, A. Yokobe, B.V. Jackson, P.L. Hick, and P.K. Manoharan, "Heliospheric Tomography Using Interplanetary Scintillation Observations 3. The Velocity Dependence of Electron Density Fluctuations in the Solar Wind", *J. Geophys. Res.*, **103**, 1991 (1998) (9 pages). +

15. Goldstein, B.E., A. Buffington, A.C. Cummings, R. Fisher, B.V. Jackson, P.C. Liewer, R.A. Mewaldt and M. Neugebauer, "Solar polar sail mission: report of a study to place a spacecraft in a polar orbit around the sun", *Proc. SPIE 3442*, 65 (1998) (12 pages).

16. Buffington, A., P. Hick, B.V. Jackson and C.M. Korendyke, "Corrals, hubcaps, and crystal balls: some new designs for very wide-angle visible-light heliospheric imagers", *Proc. SPIE 3442*, 77 (1998) (10 pages).

17. Hick, P. and B.V. Jackson, "Three-dimensional tomography of heliospheric features using Thomson-scattering data", *Proc. SPIE 3442*, 87 (1998) (7 pages). +

18. Leinert, Ch. and B.V. Jackson, "Global Heliospheric Solar Wind Changes Over Solar Cycle 21: a Comparison of Helios Photometer, In-situ and IPS data", *Astrophys. J.*, **505**, 984 (1998) (9 pages). +

19. Buffington, A., "Very-wide-angle optical systems suitable for spaceborne photometric measurements", *Applied Optics*, **37**, No. 19, 4284 (1998) (10 pages).

20. Švestka, Z., F. Farnik, H.S. Hudson and P. Hick, "Large-Scale Active Coronal Phenomena in Yohkoh SXT Images IV. Solar Wind Streams from Flaring Active Regions", *Solar Phys.*, **182**, 179 (1998) (25 pages). +

21. Webb, D.F., "The Characteristics of CMEs", in *Physics of Space Plasmas (1998) No. 15*, edited by T. Chang and J.R. Jasperse, MIT Center for Theoretical Geo/Cosmo Plasma Physics, Cambridge, MA, 337 (1998) (7 pages). +

22. Hick, P., Z.Svestka, B.V. Jackson, F. Farnik and H.S. Hudson, "Quiet Solar Wind Signatures Above Active Regions Observed in X-rays", in *Solar Wind Nine*, S.R. Habbal, R. Esser, J.V. Hollweg and P.A. Isenberg, eds., AIP Conference Proceedings 471, Woodbury, 231, (1999) (3 pages). +

23. Yokobe, A., T. Ohmi, K. Hakamada, M. Kojima, M. Tokumaru, B.V. Jackson, P.P. Hick and S. Zidowitz, "Comparison of Solar Wind Speed with Coronagraph Data Analyzed by Tomography", in *Solar Wind Nine*, S.R. Habbal, R. Esser, J.V. Hollweg and P.A. Isenberg, eds., AIP Conference Proceedings 471, Woodbury, 565, (1999) (3 pages).

24. Cliver, E., Webb, D., and Howard, R., "On the origin of solar metric type II bursts", Solar Phys., 187, 89 (1999) (26 pages).

25. Webb, D.F., "Solar Wind: Manifestations of Solar Activity", in Encyclopedia of Astronomy and Astrophysics, Inst. of Physics Publ., Bristol, UK (2000) (7 pages).

26. Jackson, B.V. and P. Hick, "Three Dimensional Tomography of Heliospheric Features Using Global Thomson Scattering Data", *Adv. in Space Res.*, **25**, No. 9, 1875, 2000. (4 pages).

27. Webb, D.F., E. Cliver, N. Crooker, O. St. Cyr, and B. Thompson, "The relationship of halo CMEs, magnetic clouds, and magnetic storms", *J. Geophys. Res.*, **105**, 7491 (2000) (18 pages). +

28. Webb, D.F. *et al.*, "The origin and development of the May 1997 magnetic cloud", *J. Geophys. Res.*, **105**, 27,251 (2000) (10 pages). +

29. Buffington, A., "Improved Design for Stray-Light Reduction with a Hemispherical Imager", *Applied Optics*, **39**, No. 16, 2683 (2000) (4 pages).

30. Webb, D.F., "Understanding CMEs and Their Source Regions", *J. Atmos. and Solar-Terr. Phys.*, **62**, 1415 (2000) (12 pages). +

31. Webb, D.F., "Coronal mass ejections: Origins, evolution and role in space weather", *IEEE Transactions of Plasma Science, Special Issue on Space Plasmas, 2000*, **28**, 1795 (2000) (12 pages). +

32. Webb, D.F., "The solar sources of geoeffective structures", *Space Weather: Progress and Challenges in Research and Applications*, edited by P. Song, G. Siscoe and H.J. Singer, **Geophys. Monograph 125**, AGU, Washington, D.C., p. 123 (2001). (19 pages)

Work In Progress:

1. Jackson, B.V., D.F. Webb, "The speeds of CMEs in the heliosphere", resubmitted to *J. Geophys. Res.* (2001) (8 pages). +

+ Acknowledges the current AF49620-97-1-0070 contract

Abstracts:

The *current* Air Force contract abstracts include:

1. Jackson, B. and P. Hick, "Two Dimensional Velocity Correlations of CME Features", AGU fall meeting, 1997, *EOS*, **78**, No. 46 Supplement, F537, (1997).

2. Lazarus, A.J., J.T. Steinberg, D.A. Biesecker, R.J. Forsyth, A,B. Galvin, F.M. Ipavich, S.E. Gibson, R.L. Lepping, A. Szabo, B.J. Thompson, K.W. Ogilvie, A. Lecinski, D.M. Hassler, P. Riley, J.T. Hoeksema, X.P. Zhao, L. Strachan, Jr., B.V. Jackson, P.J. Hick, M. Kojima, "A search for Coronal Origins of Solar Wind Streams Observed during the Whole Sun Month", AGU fall meeting, 1997, *EOS*, **78**, No. 46 Supplement, F575, (1997).

3. Webb, D.F., "Solar Mass Ejections and Recent Geoactivity". INVITED talk presented at the Boston Univ. Center for Space Physics Fall Seminar Series, Boston, 20 November 1997.

4. Webb, D., Cliver, E., Crooker N., and St. Cyr, O., "Halo CMEs and the Characteristics of Related Geoactivity", AGU fall meeting, 1997, *EOS*, **78**, No. 46 Supplement F533 (1997).

5. Yokobe, A., M. Kojima, M. Tokumaru, B.V. Jackson and P.L. Hick, "Solar Wind Speed Structure at Solar Minimum and Maximum: Tomography Analysis of Interplanetary Scintillation Observations", AGU spring meeting, 1998, *EOS*, **79**, No. 17 Supplement, S275, (1998).

6. Jackson, B.V., P. Hick, R. Howard and K. Dere, "Two-Dimensional Correlation of LASCO Images - Speeds Derived for the Background Solar Wind", AGU spring meeting, 1998, *EOS*, **79**, No. 17 Supplement, S275, (1998).

7. Webb, D.F. and J. Burkepile, "Characteristics of Magnetic Disconnection Events Associated with SMM CMEs: 1984-89". AGU spring meeting, 1998, *EOS*, **79**, No. 17 Supplement, S257 (1998).

8. Jackson, B.V., P. Hick, Ch. Leinert and A. Yokobe, "Heliospheric modeling used to map global solar wind flows", *BAAS*, **30**, No. 2, 846 (1998).

9. Hick, P., Z. Svestka, F. Farnik, H.S. Hudson and B.V. Jackson, "Fan-Like coronal X-ray Structures as Sources of the Solar Wind", *BAAS*, **30**, No. 2, 840 (1998).

10. Webb, D.F., "The Characteristics of CMEs", INVITED talk presented at the 1998 Cambridge Symposium Workshop on the Physics of Space Plasmas, Special Session on Terrestrial Consequences of Solar Eruptions, Cascais, Portugal, 23 June-2 July (1998).

11. Jackson, B.V. and P. Hick, "Three Dimensional Tomography of Heliospheric Features Using Global Thomson Scattering Data", COSPAR XXXII meeting, Nagoya, Japan, 14-19 July (1998).

12. Webb, D., C. St. Cyr and R. Howard, "Study of Magnetic Disconnection Events Associated with LASCO CMEs", COSPAR XXXII meeting, Nagoya, Japan, 14-19 July (1998).

13. Webb, D., E. Cliver, N. Crooker and C. St. Cyr, "Halo CMEs as a Predictor of Space Weather", COSPAR XXXII meeting, Nagoya, Japan, 14-19 July (1998).

14. Goldstein, B.E., A. Buffington, A.C. Cummings, R. Fisher, B.V. Jackson, P.C. Liewer, R.A. Mewaldt and M. Neugebauer, "Solar polar sail mission: report of a study to place a spacecraft in a polar orbit around the sun", to the Proceedings of the SPIE 3442 (1998).

15. Buffington, A., P. Hick, B.V. Jackson and C.M. Korendyke, "Corrals, hubcaps, and crystal balls: some new designs for very wide-angle visible-light heliospheric imagers", to the Proceedings of the SPIE 3442 (1998).

16. Jackson, B.V., A. Buffington, P. Hick, S.L. Keil, R.C. Altrock, S. Kahler, G. M. Simnett, C.J. Eyles and D. Webb, "The solar mass ejection imager (SMEI)", to the Proceedings of the SPIE 3442 (1998).

17. Hick, P. and B.V. Jackson, "Three-dimensional tomography of heliospheric features using Thomson-scattering data", to the Proceedings of the SPIE 3442 (1998).

18. Hick, P., Z. Švestka, F. Farnik, H.S. Hudson and B.V. Jackson, "Quiet solar wind signatures above active regions observed in X-rays", presented at Solar Wind 9 held on Nantucket Island, Massachussets, 5-9 October (1998).

19. Jackson, B.V., P.P. Hick, R.A. Howard and K.P. Dere, "Background coronal speeds from correlation techniques applied to LASCO images", presented at Solar Wind 9 held on Nantucket Island, Massachusetts, 5-9 October (1998).

20. Yokobe, A., M. Kojima, M. Tokumaru, B. V. Jackson, P. L. Hick and S. Zidowitz, "Comparison of Solar Wind Speed with LASCO Data Analyzed by a Tomography Method During the Whole Sun Month", presented at Solar Wind 9 held on Nantucket Island, Massachussets, 5-9 October (1998).

21. Webb, D.F., R.P. Lepping, D.E. Larson, S.F. Martin, A. Szabo, O.C. St. Cyr and B. Thompson, "January 1998 Multiple Eruption CME Event and Dual Magnetic Clouds at WIND", presented at Solar Wind 9 held on Nantucket Island, Massachussets, 5-9 October (1998).

22. Jackson, B.V., P.P Hick and A. Buffington, "Recent UCSD Advances in Tomography for Use with Heliospheric Remote-Sensing Data", *BAAS*, **31**, No. 3, 958 (1999).

23. Buffington, A., P.P. Hick and B.V. Jackson, "Visible-light All-sky Imagers in Deep Space", *BAAS*, **31**, No. 3, 959, (1999).

24. Jackson, B.V., P.P. Hick and A. Buffington, "Recent UCSD Advances in 'Time Dependent' Tomography for use with Heliospheric Remote-Sensing Data", presented at the SHINE 99 Workshop, June 14-18, (1999).

25. Webb, D.F., "Coronal Mass Ejections in the ISTP Era", presented at the AFRL/VSBS Seminar Series, April 8, (1999).

26. Webb, D.F., H.S. Hudson and J.A. Klimchuk, "Overlapping X-ray and White Light Observations of 2 CMEs with Complex Magnetic Structure". *EOS*, **79**, F710, (1998).

27. Cliver, E., N. Gopalswamy, R. Howard, C. St. Cyr and D. Webb, "Metric Type II Bursts and CMEs During the SOHO Mission". *EOS*, **79**, F712, (1998).

28. Webb, D.F., "The Variation of Solar Activity from Solar Minimum to Maximum". *EOS*, **79**, F750, INVITED (1998).

29. St. Cyr *et al.*, "SOHO LASCO/EIT Halo Coronal Mass Ejections". *EOS*, **80**, S301, (1999).

30. Webb D.F. *et al.*, "The Characteristics and Geoeffectiveness of SOHO-LASCO Halo CMEs". *BAAS*, **31**, 853, (1999).

31. Webb, D., O. St. Cyr, S. Plunkett, R. Howard, and B. Thompson, "The Characteristics and Geieffectiveness of SOHO-LASCO Halo CMEs", presented at the SHINE 99 Workshop, June 14-18 (1999).

32. Hick, P.P., B.V. Jackson, and A. Buffington, "Heliospheric Tomography: Reconstruction from Remote Sensing Observations", *EOS*, 80, F790 (1999).

33. Dunn, T, B.V. Jackson, P.P. Hick and A. Buffington, 1999, "Forecasting Solar Wind Parameters Using IPS Tomography, *EOS*, 80, F790 (1999).

34. Jackson, B.V., Hick, P.P. and Buffington, A., "Mapping Heliospheric CMEs Using Tomographic Techniques", *EOS*, 80, F810, (1999).

35. Killen, R.M., B.L. Giles, P.H. Reiff, B.V. Jackson and A. Lukyanov, "Space Weather at Mercury", *EOS*, 80, F897 (1999).

36. Webb, D.F., R.P. Lepping, L.F. Burlaga, C.E. DeForest, D.E. Larson, S.F. Martin, S.P. Plunkett, and D.M. Rust, "The origin and development of the May 1997 magnetic cloud". *EOS*, **80**, F821 (1999).

37. Webb, David, "Solar wind conditions related to the weak solar wind in May 1999". *EOS*, **80**, F857 (1999).

38. Webb, David, "Using halo CMEs to study the internal structure of CMEs". Book of Abstracts, p. 52. INVITED talk presented at the Intl. Conference on Solar Eruptive Events, Catholic Univ. of America, Washington D.C., March (2000).

39. Webb, D.F., N.U. Crooker, S.P. Plunkett, and O.C. St. Cyr, "The solar sources of geomagnetically-effective structures". Book of Abstracts, p. 43. INVITED talk presented by Webb at the Chapman Conference on Space Weather: Progress and Challenges in Research and Applications, Clearwater, FL, March (2000).

40. Webb, D.F., "Forecasting geomagnetic storms using halo CMEs". Book of Abstracts, p. 55. Presented by Webb at the Chapman Conference on Space Weather: Progress and Challenges in Research and Applications, Clearwater, FL, March (2000).

41. Jackson, B.V. and P.P Hick, "Time Dependent Tomography of Heliospheric Features Using Global Thomson-Scattering Data From the Helios Spacecraft Photometers During Times of Solar Maximum", *EOS*, **81**, S353 (2000) (1 page).

42. Jackson, B.V. and P.P. Hick, "Time-Dependent Tomography Of Heliospheric Features Using Global Thomson-Scattering Data From the Helios Spacecraft Photometers'", presented at the SHINE 2000 Workshop, June 14-17, (2000) (1 page).

43. Hick, P.P., B.V. Jackson and A. Buffington, "Prediction of Solar Wind Conditions in the Inner Heliosphere Using IPS Tomography"', *BAAS*, **32**, 818, (2000) (1 page).

44. Jackson, B.V. and P.P. Hick, ``Time-Dependent Tomography Of Heliospheric Features Using Global Thomson-Scattering Data From the Helios Spacecraft Photometers", *BAAS*, **32**, 829, (2000) (1 page).

45. Webb, D.F., R.P. Lepping, N.U. Crooker, S.P. Plunkett, and O.C. St. Cyr, "Studying CMEs using LASCO and in-situ observations of halo events". *BAAS*, **32**, 825, (2000).

46. Space Weather write-up in UniSci (Daily University Science News) June 6, 2000.

47. Space Com News write-up and citation June 10, 2000 at: http://www.space.com/scienceastronomy/solarsystem/solar_eruption_000612.html

48. Space Weather write-up in AScribe, the public interest newswire, June 14, 2000.

49. Jackson, B.V. and P.P. Hick, "Space Weather Using Remote Sensing Observations", to the NASA Applied Information Systems Research Program (AISRP) 2000 Workshop held in Boulder, Colorado 20-22 September (2000) (1 page).

50. Hick, P.P. and B.V. Jackson, "Visualization of Remotely-Sensed Heliospheric Plasmas", to the NASA Applied Information Systems Research Program (AISRP) 2000 Workshop held in Boulder, Colorado 20-22 September (2000) (1 page).

51. New Scientist news article write-up, ``Wicked weather", 5 August 2000, p. 36, by Eugenie Samuel (4 pages).

52. Webb, D. F., "Halo CMEs and Space Weather". Book of Abstracts, p. 24. INVITED talk presented by Webb at the UVCS/SOHO 2000 Science Meeting, Northeast Harbor, ME, September (2000).

53. Jackson, B.V. and Hick, P.P., "Real-Time Heliospheric Forecasting -- Three-Dimensional Reconstruction of Heliospheric Features Using Remote-Sensing Data", *The First S-RAMP Conference Abstracts*, 96, SRAMP 2000, Sapporo, Japan, October 1 - 6 (2000) (1 page).

54. Jackson, B.V., Hick, P.P. and Buffington, A., "The Best Use of Heliospheric Photometric Images -- Time-Dependent Tomography of Heliospheric Features Using Global Thomson-Scattering Data", *The First S-RAMP Conference Abstracts*, 423, SRAMP 2000, Sapporo, Japan, October 1 - 6 (2000) (1 page).

55. Webb, D., R. Lepping, S. Plunkett, and S.-T. Wu, "Relationship of the Apr. 29, 1998 Halo CME and the Magnetic Cloud and Geoactivity on May 2-3". *The First S-RAMP Conference Abstracts*, 43, SRAMP 2000, Sapporo, Japan, October 1 - 6 (2000).

56. Webb, D., "Solar Sources of Geoactivity During September – October 1999". *The First S-RAMP Conference Abstracts*, 439, SRAMP 2000, Sapporo, Japan, October 1 - 6 (2000).

57. Jackson, B.V., "CMEs in Three Dimensions – Techniques Used in Their Tomographic Analyses", *EOS*, **81**, F979 (2000) (1 page).

58. St. Cyr, O.C., J.T. Burkepile, D.F. Webb, B.V. Jackson and R.A. Howard, "White Light Measurements of the Radial Extent of CMEs". *EOS*, **81**, F978 (2000).

59. Zhao, X. and D.F. Webb, "Large-Scale Closed Field Regions and Halo Coronal Mass Ejections". *EOS*, **81**, F975 (2000).

III.F. UCSD Personnel Supported by this Contract

B. Jackson - Research Physicist

A. Buffington - Research Physicist

P. Hick – Assistant Research Physicist

D. Webb – Research Physicist under subcontract to Boston College

A. Yokobe, T. Ohmi – graduate students

J. Copps, T. Dunn, J. Chao – students

IV. Conclusion

Solar disturbances produce major effects in the corona, its extension into the interplanetary medium, and ultimately, the Earth's environment. The ability to forecast the arrival at Earth of these disturbances and to determine their effects on the geospace environment is of primary interest to the Air Force, which communicates through and maintains satellites within this environment. We have developed imaging and other techniques for use in mapping these disturbances (mainly coronal mass ejections or CMEs) as they move away from the Sun. This capability has begun to revolutionize the study of large-scale heliospheric space plasma interactions.

The Solar Mass Ejection Imager (SMEI), now being developed and constructed, will have an angular and temporal resolution far better than the data sets (interplanetary scintillation and Thomson scattering observations from the HELIOS photometers) for which our imaging techniques were originally developed. SMEI will produce a thousand times as much data as previously available, exceeding our current data analysis capabilities. We have developed the algorithms for SMEI data analysis and model development. We have tested these algorithms using data obtained from a ground-based prototype SMEI optical system. Furthermore, we have also created imaging and analysis tools adapted specifically for use with SMEI observations.

An important requirement for the efficient analysis of SMEI observations will be the ability to trace solar plasma changes near Earth and elsewhere in the interplanetary medium in three

dimensions, thereby enabling us to model and study the physics of heliospheric disturbances from a three-dimensional perspective. The development of adequate analysis and modeling techniques for SMEI data is a serious challenge, which must be addressed in order to maximize the scientific return from the SMEI mission, in particular with respect to our ability to accurately forecast the arrival of heliospheric disturbances at Earth.

References:

Ananthakrishnan, S., Coles, W.A. and Kaufman, J.J., 1980, *J. Geophys. Res.*, **85**, 6025.

Antiochos, S.K., DeVore, C.R. and Klimchuk, J.A., 1999, *Astrophys. J.*, **510**, 485.

Asai, K., Kojima, M., Tokumaru, M., Yokobe, A., Jackson, B.V., Hick, P.L., and Manoharan, P.K., 1998, *J. Geophys. Res.*, **103**, 1991.

Behannon, K.W, Burlaga, L.F. and Hewish, A., 1991, *J. Geophys. Res.*, **96**, 21,213.

Buffington, A., 1998, *Applied Optics*, **37**, No. 19, 4284.

Buffington, A., 2000, *Applied Optics*, **39**, No. 16, 2683.

Buffington, A., Jackson, B.V., and Korendyke, C.M, 1996, *Appl. Optics* **35**, 6669.

Buffington, A., Hick, P., Jackson B.V., and Korendyke, C.M., 1998, *Proc. SPIE 3442*, 77.

Burlaga, L.F., 1991, in R. Schwenn and E. Marsch eds., *Physics of the Inner Heliosphere, Vol. 2: Particles, Waves and Turbulence*, Springer, Berlin., p. 1.

Burlaga, L., Sittler, E., Mariani, F., and Schwenn, R., 1981, *J. Geophys. Res.* **86**, 6673.

Burlaga, L.F., C.W. Smith, R.M. Skoug, D.F. Webb, T.H. Zurbuchen, and A. Reinard, 2001, *J. Geophys. Res.*, **106**, 20,957.

Chen, J. and 9 coauthors, *Astrophys. J.*, 1997, **490**, L191.

Chen, J., Santoro, R.A., Krall, J., Howard, R.A., Duffin, R., Moses, J.D., Brueckner, G.E., Darnell, J.A. and Burkepile, J.T., 2000, *Astrophys. J.*, **533**, 481.

Crooker, N.U., Siscoe, G.L., Shodhan, S., Webb, D.F., Gosling, J.T. and Smith, E.J., 1993, *J. Geophys. Res.*, **98**, 9371.

Fisher, R. and Sime, D.G., 1984, *Astrophys. J.*, **285**, 354.

Gapper, G.R., Hewish, A., Purvis, A. and Duffett-Smith, P.J., 1982, *Nature*, **296**, 633.

Gosling, J.T., 1990, in C.T. Russell, E.R. Priest and L.C. Lee (eds.), *Physics of Magnetic Flux Ropes*, Geophys. Monogr. Ser., **58**, p. 343.

Hewish, A and Bravo, S., 1986, *Solar Phys.*, **106**, 185.

Hewish, A., Scott, P.F. and Wills, D., 1964, *Nature*, **203**, 1214.

Hick, P. and Jackson, B., 1994, *Adv. in Space Res.*, **14**, 135.

Hick, P. and Jackson, B.V., 1998, *Proc. SPIE 3442*, 87.

Hick, P., Jackson, B.V. and Schwenn, R., 1990, *Astron. Astrophys.* **285**, 1.

Hick, P.L., Jackson, B.V. and Schwenn, R., 1992, in *Solar Wind Seven*, E. Marsch and R. Schwenn, eds., Pergamon, Oxford, 187.

Hick, P., Jackson, B.V., Altrock, R.C., Woan,G. and Slater, G., 1995a, *Adv. in Space Res.*, **17**, 311.

Hick, P., Jackson, B.V., Rappoport, S., Woan, G., Slater, G., Strong, K., and Uchita, Y., 1995b, *Geophys. Res. Lett.*, **22**, 643.

Hick, P., Jackson B.V., and Altrock, R., 1995c, in *Solar Wind Eight*, D. Winterhalter, J.T.Gosling, S.R. Habbal, W.S. Kurth and M. Neugebauer, eds., AIP Conference Proceedings 382, Woodbury, 169.

Hick, P., Švestka, Z, Farnik, F., Hudson H.S., and Jackson, B.V., 1999, in *Solar Wind Nine*, S.R. Habbal, R. Esser, J.V. Hollweg and P.A. Isenberg, eds., AIP Conference Proceedings 471, Woodbury, 231.

Hoeksema, J.T., Wilcox, J.M. and Scherrer, P.H., 1983, *J. Geophys. Res.*, **88**, 9910.

Howard, R.A. et al., 1997, in *Coronal Mass Ejections,* **GM vol. 99**, N. Crooker, J. Joselyn and J. Feynman, eds., p. 17, AGU, Washington, DC.

Houminer, Z., 1971, *Nature Phys. Sci.*, **231**, 165.

Hudson, H.S., J.R. Lemen, O.C. St. Cyr, A.C. Sterling, and D.F. Webb, 1998, *Geophys. Res. Lett.*, **25**, 2481.

Jackson, B.V., 1981, *Solar Phys.*, **73**, 133.

Jackson, B.V., 1985a, *Solar Phys.*, **95**, 363.

Jackson, B.V., 1985b, *Solar Phys.*, **100**, 563.

Jackson, B.V., 1989, *Adv. Space Res.*, **9**, 69.

Jackson, B.V., 1991a, *J. Geophys. Res.*, **96**, 11,307.

Jackson, B.V., 1991b, in Proceedings of the First SOLTIP Symposium held in Liblice, Czechoslovakia 30 September - 5 October, S. Fischer and M. Vandas, eds., Astronomical Institute of the Czechoslovak Academy of Sciences, Prague, 153.

Jackson, B.V., 1997, in *Magnetic Storms*, Geophysical Monograph Series, **98**, W. Gonzalez, Y. Kamide and B. Tsurutani, eds., 59.

Jackson, B.V. and Leinert, C., 1985, *J. Geophys. Res.*, **90**, 10,759.

Jackson, B.V. and Hick, P.L., 1994, in the proceedings of the Third SOHO Workshop on Solar Dynamic Phenomena & Solar Wind Consequences, **ESA SP-373**, 199.

Jackson, B.V. and Webb, D.F., 1994, in the proceedings of the Third SOHO Workshop on Solar Dynamic Phenomena & Solar Wind Consequences, **ESA SP-373**, 233.

Jackson, B.V. and Froehling, H.R., 1995, *Astron. Astrophys.*, **299**, 885.

Jackson, B.V. and Hick, P., 2000, *Adv. in Space Res.*, **25**, No. 9, 1875.

Jackson, B.V. and Webb, D.F., 2001, in preparation to be submitted to *J. Geophys. Res.*

Jackson, B.V., Howard, R.A., Sheeley, N.R., Jr., Michels, D.J., Koomen, M.J., and Illing, R.M.E., 1985, *J. Geophys. Res.*, **90**, 5075.

Jackson, B.V., Rompolt, B. and Švestka, Z., 1988, *Solar Phys.*, **115**, 327.

Jackson, B.V., H.S. Hudson, J.D. Nichols and R.E. Gold, 1989, in *Solar System Plasma Physics Geophysical Monograph*, **54** J.H. Waite, Jr, J.L. Burch and R.L. Moore, eds., 291.

Jackson, B., R. Gold and R. Altrock, 1991, *Adv. in Space Res.*, **11**, 377.

Jackson, B.V., Hick, P.L. and Webb, D.F., 1993, *Adv. in Space Res.*, **13**, 43.

Jackson, B.V., Webb, D.F., Hick, P.L. and Nelson, J.L., 1994, *PL-TR-94-2040, Scientific Report No. 4*, Phillips Laboratory, Hanscom.

Jackson, B.V., A. Buffington, P.L. Hick, S.W. Kahler, R.C. Altrock, R.E. Gold and D.F. Webb, 1995, in *Solar Wind Eight*, D. Winterhalter, J.T.Gosling, S.R. Habbal, W.S. Kurth and M. Neugebauer, eds., AIP Conference Proceedings 382, Woodbury, 536.

Jackson, B.V., Hick, P.L., Kojima, M. and Yokobe, A, 1997a, *Physics and Chemistry of the Earth*, **22**, No. 5, 425.

Jackson, B.V., A. Buffington, P.L. Hick, S.W. Kahler, G. Simnett and D.F. Webb, 1997b, *Physics and Chemistry of the Earth*, **22**, No. 5, 441.

Jackson, B.V., Hick, P.L., Kojima, M. and Yokobe, A., 1997c, for the COSPAR XXXI meeting held in Birmingham, England 14-21 July, 1996 *Adv. in Space Res.*, **20**, No. 1, 23.

Jackson, B.V., Hick, P.L., Kojima, M. and Yokobe, A., 1998, *J. Geophys. Res.*, **103**, 12,049.

Jackson, B.V., Hick, P.P. and Buffington, A., 1999a, "Recent UCSD Advances in Tomography for Use with Heliospheric Remote-Sensing Data", *BAAS*, **31**, No. 3, 958.

Jackson, B.V., P.P. Hick and A. Buffington, 1999b, "Recent UCSD Advances in 'Time Dependent' Tomography for use with Heliospheric Remote-Sensing Data", presented at the SHINE 99 Workshop, June 14-18.

Kahler, S.W., 1977, *Astrophys. J.*, **214**, 891.

Kahler, S.W., Hildner, E. and van Hollebeke, M.A.I., 1978, *Solar Phys.*, **57**, 429.

Keil, S.L, Altrock, R.C., Kahler, S.W., Jackson, B.V., Buffington, A., Hick, P.L., Simnett, G., Eyles, C., Webb, D.F. and Anderson, P., 1996, Denver 96 "Missions to The Sun", *SPIE 2804*, 78.

Kojima, M., Asai, K., Jackson, B.V., Hick, P.L., Tokumaru, M., Watanabe, H., Yokobe, A. and Manoharan, P.K., 1997, in *Robotic exploration close to the Sun: Scientific Basis*, S.R. Habbal, ed., AIP Conference proceedings 385, New York, 97.

Kojima, M., Tokumaru, M., Watanabe, H., Yokobe, A., Asai, K., Jackson, B.V., and Hick, P.L., 1998, *J. Geophys. Res.*, **103**, 1981.

Leinert, Ch. and Jackson, B.V., 1998, *Astrophys. J.*, **505**, 984.

Leinert, C., Link, H. and Salm, N., 1981, *J. Space Sci. Instr.*, **5**, 257.

Lin, J. and T.G. Forbes, 2000, *J. Geophys. Res.*, **105**, 2375.

Richter, I., Leinert, C. and Planck, B., 1982, *Astron. Astrophys.*, **110**, 115.

Rickett B.J., and Coles, W.A., 1991, *J. Geophys. Res.*, **96**, 1717.

Rust, D.M., Hildner, E. and 11 co-authors, 1980, Introduction in *Solar Flares, A Monograph from Skylab Solar Workshop II* (ed. P.A. Sturrock), Colorado Associated Press.

Schwenn, R., 1986, *Space Sci. Revs.*, **44**, 139.

Sheeley, N.R., Jr., Howard, R.A. and Michels, D.J., 1983, *Astrophys. J.*, **272**, 349.

St. Cyr, O.C, *et al.*, 2000, *J. Geophys. Res.*, **105**, 18,169.

Švestka, Z., 1981, in E.R. Priest (ed), *Flare Magnetohydrodynamics* (Gordon and Breach), p. 47.

Švestka, Z, 1986, in D.F. Neidig (ed.), *Proceedings of the NSO/SMM Symposium: The Lower Atmosphere of Solar Flares*, p. 332.

Švestka, Z., Farnik, F., Hudson H.S., and Hick, P., 1997, in A. Wilson (ed.), 31st ESTLAB Symposium: *Correlated Phenomena at the Sun, in the Heliosphere and in Geospace*, ESA SP-415, ESTEC, Noordwijk, Netherlands, p. 139.

Švestka, Z., F. Farnik, H.S. Hudson and P. Hick, 1998, *Solar Phys.*, **182**, 179.

Tsurutani, B.T., Gonzales, W.D., Gonzales, A.L.C., Tang, F., Araballo, J.K. and Okada, M., 1995, *J. Geophys. Res.*, **100**, 21,717.

Vourlidas, A., Subramanian, P., Dere K., and Howard, R., 2000, *Astrophys. J.*, **534**, 456.

Webb, D.F., 1997a, in a SHINE report to the ISTP program, at:
http://umbra.nascom.nasa.gov/istp/SHINE_report.html.

Webb, D.F., 1997b, INVITED talk presented at the Boston Univ. Center for Space Physics Fall Seminar Series, Boston, 20 November 1997.

Webb, D.E. and Kundu, M., 1978, *Solar Phys.*, **57**, 155.

Webb, D.F. and Jackson, B.V., 1992, in *Solar Wind Seven*, E. Marsch and R. Schwenn, eds., Pergamon, Oxford, 681.

Webb, D.F. and Jackson, B.V., 1993, in the *Solar Terrestrial Predictions Workshop 4* in Ottawa, Canada 18 - 22 May, A. Huruska *et al.* eds., NOAA, Boulder, 381.

Webb, D.F. and Howard, R.A., 1994, *J. Geophys. Res.*, **99**, 4201.

Webb, D.F. and Jackson, B.V., 1996, presentation at the COSPAR XXXI meeting, Birmingham, England 14-21 July, 1996.

Webb, D.F. and Burkepile, J, 1998. *EOS*, **79**, S257.

Webb, D.E., Cheng, C.C., Dulk, G.A., Edberg, S.J., Martin, S.F., McKenna-Lawlor, S. and McLean, D.J., 1980, in *Solar Flares, A Monograph from Skylab Solar Workshop II* P.A. Sturrock, ed., Colorado Associated Press, 471.

Webb, D.F., Jackson, B.V., Hick, P., Schwenn, R., Bothmer, V. and Reames, D., 1993a, *Adv. in Space Res.*, **13**, 71.